Analysis of Tests of Subsurface Injection, Storage, and Recovery of Freshwater in the Lower Floridan Aquifer, Okeechobee County, Florida

U.S. GEOLOGICAL SURVEY

Open-File Report 95-765

Prepared in cooperation with the
SOUTH FLORIDA WATER MANAGEMENT DISTRICT

Analysis of Tests of Subsurface Injection, Storage, and Recovery of Freshwater in the Lower Floridan Aquifer, Okeechobee County, Florida

By Vicente Quiñones-Aponte, Kevin Kotun, and Joseph F. Whitley

U.S. GEOLOGICAL SURVEY

Open-File Report 95-765

Prepared in cooperation with the

South Florida Water Management District

Tallahassee, Florida
1996

U.S. DEPARTMENT OF THE INTERIOR
BRUCE BABBITT, Secretary

U.S. GEOLOGICAL SURVEY
Gordon P. Eaton, Director

For additional information, write to:

District Chief
U.S. Geological Survey
Suite 3015
227 N. Bronough Street
Tallahassee, Florida 32301

Copies of this report can be purchased from:

U.S. Geological Survey
Earth Science Information Center
Open-File Reports Section
Box 25286, MS 517
Denver, CO 80225

CONTENTS

FIGURES

TABLES

GLOSSARY OF TERMS

A	Area [L^2]
A_{eff}	Effective area [L^2]
b	Thickness of the flow zone [L]
C	Solute concentration [M/L^3]
C_i	Solute concentration in injected water [M/L^3]
C_n	Solute concentration in native water [M/L^3]
c	Volumetric solute concentration in the aquifer fluid [M/L^3]
c'	Volumetric solute concentration in the injected fluid [M/L^3]
D_d	Molecular diffusion coefficient [L^2/T]
$\underline{D}_m$	Dispersion tensor [L^2/T]
d	Characteristic length [L]
dh_i	Head change in the *i-th* high-permeability zone [L]
d_r	Change in distance from the pumping well [L]
g	Gravitational acceleration vector [L/T^2]
$\underline{I}$	Identity tensor [dimensionless
K_i	Hydraulic conductivity of the *i-th* high-permeability zone [L/T]
k	Intrinsic permeability of the aquifer [L^2]
k_H	Horizontal permeability of the aquifer material [L^2]
k_V	Vertical permeability of the aquifer material [L^2]
n	Apparent porosity of the aquifer [dimensionless]
p	Fluid pressure [M/LT^2]
ρ	Fluid density [M/L^3]
ρ_i	Density of injected water [M/L^3]
ρ_n	Density of native water [M/L^3]
Pgh	Hydrostatic pressure [M/LT^2]
Q	Flow rate through the flow zone [L^3/T]
Q'	Volumetric injection rate per unit area of aquifer [L/T]
Q_i	Representation of flow components from the different aquifer high-permeability zones where $i = 1,2,3$ [L^3/T]
Q_p	Mass of fluid injected or withdrawn per unit time per unit volume of aquifer [M/L^3T]
Q_T	Total flow rate through the well [L^3/T]
q	Specific discharge [L/T]
R_e	Reynolds number [dimensionless]
r	Radial distance [L]
T_i	Transmissivity of the aquifer [L^2/T]
t	Time [T]
μ	Dynamic viscosity of the fluid [M/LT]
V	Fluid kinematic viscosity [L^2/T]
v	Average pore-water velocity [L/T]
z	Elevation above a reference datum [L]
α_L	Longitudinal dispersivity of the aquifer [L]
α_T	Transverse dispersivity of the aquifer [L]
Δt	Time step [T]
∇	Gradient operator [1/L]

Analysis of Tests of Subsurface Injection, Storage, and Recovery of Freshwater in the Lower Floridan Aquifer, Okeechobee County, Florida

By Vicente Quiñones-Aponte, Kevin Kotun, *and* Joseph F. Whitley

Abstract

A series of freshwater subsurface injection, storage, and recovery tests were conducted at an injection-well site near Lake Okeechobee in Okeechobee County, Florida, to assess the recoverability of injected canal water from the Lower Floridan aquifer. At the study site, the Lower Floridan aquifer is characterized as having four local, relatively independent, high-permeability flow zones (389 to 398 meters, 419 to 424 meters, 456 to 462 meters, and 472 to 476 meters below sea level). Four subsurface injection, storage, and recovery cycles were performed at the Lake Okeechobee injection-well site in which volumes of water injected ranged from about 387,275 to 1,343,675 cubic meters for all the cycles, and volumes of water recovered ranged from about 106,200 to 484,400 cubic meters for cycles 1, 2, and 3. The recovery efficiency for successive cycles 2 and 3 increased from 22 to 36 percent and is expected to continue increasing with additional cycles.

A comparison of chloride concentration breakthrough curves at the deep monitor well (located about 171 meters from the injection well) for cycles 1, 4, and test no. 4 (from a previous study) revealed unexpected findings. One significant result was that the concentration asymptote, expected to be reached at concentration levels equivalent or close to the injected water concentration, was instead reached at higher concentration levels. The injection to recovery rate ratio might affect the chloride concentration breakthrough curve at the deep monitor well, which could explain this unexpected behavior. Because there are four high-permeability zones, if the rate of injection is smaller than the rate of recovery (natural artesian flow), the head differential might not be transmitted through the entire open wellbore, and injected water would probably flow only through the upper high-permeability zones. Therefore, observed chloride concentration values at the deep monitor well would be higher than the concentration of the injected water and would represent a mix of water from the different high-permeability zones.

A generalized digital model was constructed to simulate the subsurface injection, storage, and recovery of freshwater in the Lower Floridan aquifer at the Lake Okeechobee injection-well site. The model was constructed using a modified version of the Saturated-Unsaturated **TRA**nsport code (SUTRA), which simulates variable-density advective-dispersive solute transport and variable-density ground-water flow. Satisfactory comparisons of simulated to observed dimensionless chloride concentrations for the deep monitor well were obtained when using the model during the injection and recovery phases of cycle 1, but not for the injection well during the recovery phase of cycle 1 even after several attempts. This precluded the determination of the recovery efficiency values by using the model.

The unsatisfactory comparisons of simulated to observed dimensionless chloride concentrations for the injection well and failure of the model to represent the field data at this well could

be due to the characteristics of the Lower Floridan aquifer (at the local scale), which is cavernous or conduit in nature. To test this possibility, Reynolds numbers were estimated at varying distances from the injection well, taking into consideration two aquifer types or conceptual systems, porous media and cavernous. For the porous media conceptual system, the Reynolds numbers were greater than 10 at distances less than 1.42 meters from the injection well. Thus, application of Darcy's law to ground-water flow might not be valid at this distance. However, at the deep monitor well (171 meters from the injection well), the Reynolds number was 0.08 which is indicative of laminar porous media flow. For the cavernous conceptual system, the Reynolds numbers were greater than 2,000 at distances less than 1,000 meters from the well. This number represents the upper limit of laminar flow, which is the fundamental assumption for the application of Darcy's law to free flow.

Results from the study suggest that to simulate recovery efficiency for the Lower Floridan aquifer at the Lake Okeechobee injection-well site might require the application of a free-flow type model (conduit flow or fracture flow). This type of model may produce a more realistic representation of the actual fluid motion in the Lower Floridan aquifer and could provide appropriate estimates of the recovery efficiency.

INTRODUCTION

Lake Okeechobee is the second largest natural freshwater lake in the United States, encompassing about 1,813 km^2 (square kilometers). The lake is the principal source of potable water for southern Florida and is part of the flood-control system for the area (fig. 1). A serious contamination problem to Lake Okeechobee is posed by phosphate loads from tributary canals, such as Taylor Creek and Nubbin Slough (fig. 1), which might accelerate eutrophication of the lake (Lake Okeechobee Technical Advisory Committee, 1986). The Lake Okeechobee Technical Advisory Committee proposed a study to determine the feasibility of reducing phosphate loads into Lake Okeechobee.

From April 1991 to September 1994, the U.S. Geological Survey, in cooperation with the South Florida Water Management District, conducted a study to: (1) assess the feasibility of subsurface injection, storage, and recovery as a mechanism for reducing phosphate loads in the canal water; (2) examine the chemical behavior of the canal-water and native aquifer water mix during subsurface injection, storage, and recovery, focusing on the fate of orthophosphate; and (3) estimate the recovery efficiency of injected canal water from the Lower Floridan aquifer. A report by Quiñones-Aponte and Whitley (1996, in press) analyzed the application of phosphate mass-balance approaches to assess the feasibility of subsurface injection, storage, and recovery as a tool for reducing phosphate loads in the canal water. This report assesses the recoverability of injected canal water from the Lower Floridan aquifer.

Purpose and Scope

The purposes of this report are to: (1) describe a series of freshwater subsurface injection, storage, and recovery tests conducted at an injection-well facility near Lake Okeechobee; (2) present the analyses of the subsurface injection, storage, and recovery tests; and (3) assess the recoverability of injected canal water from the Lower Floridan aquifer using field data and digital model analyses. This report combines information and results from a previous study (CH_2M Hill, 1989) and the present study to characterize the Lower Floridan aquifer at the Lake Okeechobee injection-well site; these characteristics include lithostratigraphic units, hydrogeologic units, aquifer properties, potentiometric levels, and ambient water quality. Recovery efficiencies from actual field subsurface injection, storage, and recovery tests were estimated and are included in this report to measure the success of a subsurface injection, storage, and recovery cycle. A summary of the governing ground-water flow and solute transport equations is also included with a description of the digital model development and its application to evaluate recovery efficiency at the Lake Okeechobee injection-well site. Finally, simulations were made using a digital model code (QSUTRA) to study the effects of the aquifer characteristics on the recoverability of the injected canal water.

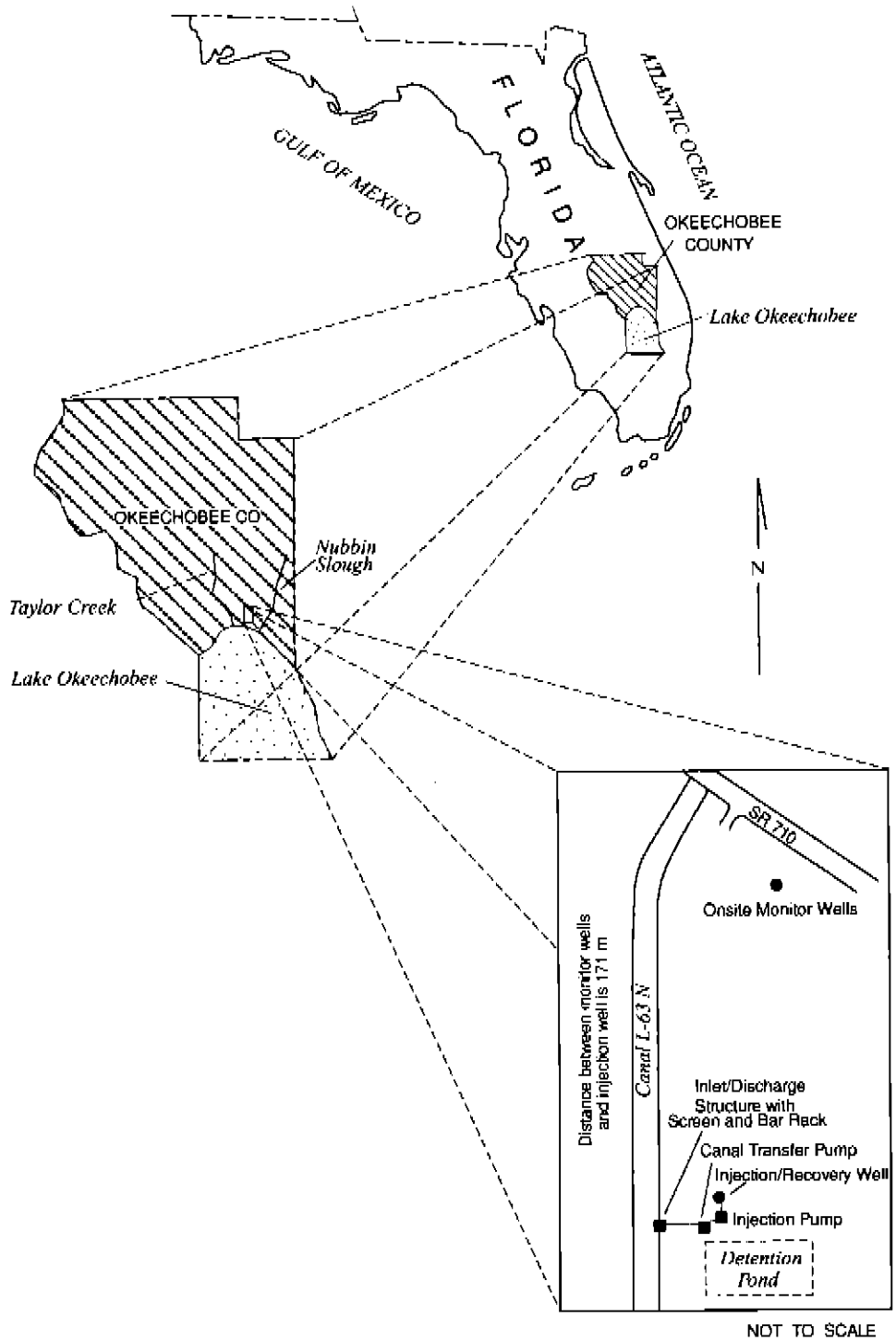

Figure 1. Location of the Lake Okeechobee injection-well site and the contributing canals.

Description of Study Area

The study area is located at existing well facilities near the northern shore of Lake Okeechobee at the intersection of State Road 710 and Canal L-63N in Okeechobee County, Fla. (fig. 1). The facilities were designed and constructed by CH_2M Hill (1989), under an agreement with the South Florida Water Management District, and consist of a canal inlet/discharge structure to withdraw water from Canal L-63N, chlorination facilities (not used for the present study), a detention pond, an injection well, pumps, and two nested monitor wells located about 171 m (meters) from the injection well (fig. 1). All the wells are characterized by artesian heads. Initial testing at this well site was conducted by CH_2M Hill (1989).

The general hydrogeologic characteristics of the injection well site are briefly described in the subsequent sections, including lithostratigraphic and hydrogeologic units. The description of the aquifer hydraulic characteristics focuses on the Lower Floridan aquifer, which is the hydrogeologic unit considered in this study.

Hydrogeologic Setting

The geology of Okeechobee County and the Lake Okeechobee injection-well site has been described by previous investigators, including Sellards (1912), Parker and others (1955), Puri and Vernon (1964), Miller (1986), CH_2M Hill (1989), and Lukasiewicz (1992). The upper 550 m of sediments at the injection-well site are comprised of the upper part of the Oldsmar Formation of lower Eocene age, the Avon Park Formation (formerly termed the Lake City Limestone) of middle Eocene age, the Ocala Limestone of upper Eocene age, the Tampa Limestone of Miocene age, the Hawthorn Formation of Miocene age, the Tamiami Formation of Pliocene age, and the Anastasia Formation of Pleistocene age (fig. 2).

The Oldsmar Formation, Avon Park Formation, and Ocala Limestone are present in the Floridan aquifer system (fig. 2). The Ocala Limestone and the upper part of the Avon Park Formation constitute the Upper Floridan aquifer, the middle part of the Avon Park Formation constitutes the middle semiconfining unit, and the lower part of the Avon Park Formation and the upper part of the Oldsmar Formation constitute the Lower Floridan aquifer (Miller, 1986). The middle semiconfining unit separates the Upper Floridan aquifer from the Lower Floridan aquifer within the Floridan aquifer system. The Oldsmar Formation is characterized by off-white to light-gray, micritic to finely pelletal limestone interbedded with gray to tan to light-brown, fine to medium crystalline, commonly vuggy dolomite (Miller, 1986). The Avon Park Formation is characterized by pelletal but locally micritic cream, tan, or light-brown, soft to well-indurated limestone sediments (Miller, 1986) with fauna typical of Eocene age and also contains large amounts of lignite and carbonaceous plant material (Puri and Vernon, 1964). Overlying the Avon Park Formation is the Ocala Limestone containing marine fauna and foraminifera throughout and chert beds in places. The cavernous Ocala Limestone produces large volumes of water and is the source of many springs in Florida that originate from the Floridan aquifer system (Parker and others, 1955).

The Tampa Limestone and Hawthorn Formation are present in a confining unit (about 162 m thick) between the surficial aquifer and the Floridan aquifer system (fig. 2) and consist of sand, silts, and limestones of marine origin. Limestones are predominant in the lower part of the Tampa Limestone (Puri and Vernon, 1964). At the Lake Okeechobee injection-well site, the Tampa Limestone is characterized as a soft loosely consolidated limestone, rich in phosphorite (fig. 2). The base of the Tampa Limestone is considered the top of the Floridan aquifer system and is identified by increased consolidation and occurrence of arenaceous limestone. The Hawthorn Formation overlying the Tampa Limestone contains many types of deposits, including carbonate with quartz sand and phosphatic clayey dolostones. The Tamiami Formation and Anastasia Formation are present in the surficial aquifer (fig. 2). At the Lake Okeechobee injection-well site, the Tamiami Formation consists of fine silty sand, shell fragments, low phosphorite, and interbedded clay (CH_2M Hill, 1989). The Anastasia Formation is generally composed of coquina, quartz sand, calcareous quartz sandstone, and shelly marl (Sellards, 1912) but consists of unconsolidated sand with fine shell fragments at the injection-well site (CH_2M Hill, 1989).

Hydraulic Characteristics of the Lower Floridan Aquifer

The Lower Floridan aquifer at the Lake Okeechobee injection-well site is characterized by two flow zones under confined conditions isolated from each other by an intermediate dolomite confining unit (CH_2M Hill, 1989; and Lukasiewicz, 1992). The upper

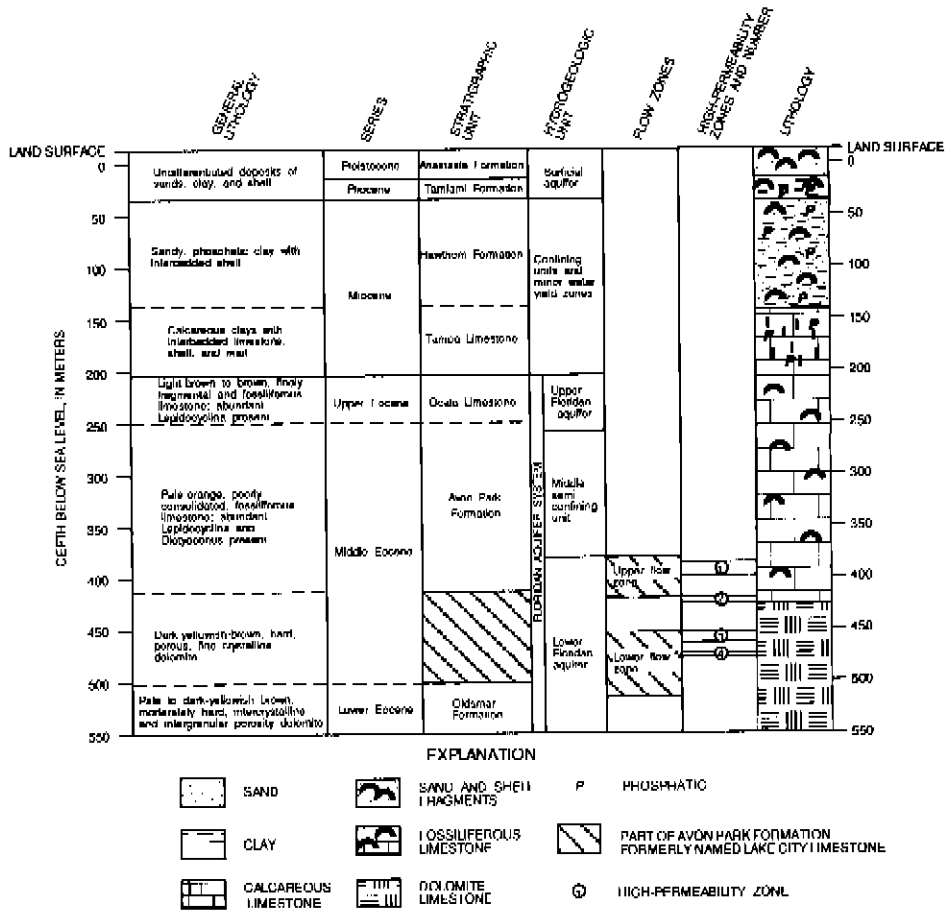

Figure 2. Geologic column of the Lake Okeechobee injection-well site showing stratigraphic units, hydrogeologic units, and lithology. Modified from CH_2M Hill (1989).

flow zone occurs from about 380 to 419 m below sea level, the intermediate confining unit occurs from about 419 to 456 m below sea level, and the lower flow zone occurs from about 456 to 518 m below sea level (fig. 2). At local scale, high-permeability zones occur along some intervals in the upper and lower flow zones (CH_2M Hill, 1989). Local high-permeability zones were present along two intervals in the upper flow zone (389 to 398 m below sea level and 419 to 424 m below sea level) and along two intervals in the lower flow zone (456 to 462 m below sea level and 472 to 476 m below sea level).

Field data and model simulation results from Lukasiewicz (1992) were used to estimate the direction and magnitude of the regional ground-water flow gradient at the Lake Okeechobee injection-well site. The direction of flow was estimated at about 45 degrees northeast from true north and the background hydraulic gradient was about 0.047 m/km (meter per kilometer). The four local high-permeability zones occurring within the upper and lower flow zones were identified by CH_2M Hill (1989) using data from geophysical logs (caliper, flow velocity, fluid resistivity, and fluid temperature) during pumping conditions. The percent of flow from the individual local high-permeability zones (table 1) was estimated from caliper/velocity (flow meter) borehole logs conducted during pumping or flowing conditions (CH_2M Hill, 1989).

CH_2M Hill (1989) estimated the hydraulic characteristics of the open-hole interval of the injection well and the middle semiconfining unit above the flow zones. The estimated transmissivity of the aquifer at the injection well was about 71,000 m^2/d (meters squared per day) for the interval between 377 and 509 m below sea level, which is equivalent to an average hydraulic conductivity of 540 m/d (meters per day).

Table 1. Hydraulic characteristics of the Lower Floridan aquifer at the Lake Okeechobee injection-well site

[Percent of flow estimated using caliper and flow-meter borehole logs]

High-permeability zone	Depth interval (meters below sea level)	Thickness (meters)	Percent of flow from this zone	Horizontal hydraulic conductivity (meters per second)	Horizontal intrinsic permeability (square meters)
1	389-398	9.0	60	5.48×10^{-2}	5.57×10^{-9}
2	419-424	5.0	11	1.81×10^{-2}	1.84×10^{-9}
3	456-462	6.0	22	3.01×10^{-2}	3.06×10^{-9}
4	472-476	4.0	7	1.44×10^{-2}	1.46×10^{-9}

The hydraulic characteristics of the middle semiconfining unit were estimated from a packer test conducted at a depth interval of between 349 and 365 m below sea level. This middle semiconfining unit (fig. 2) confines the aquifer considered in the subject study at its upper limit. Transmissivity values in this unit ranged from 65.6 to 273.2 m^2/d, which is equivalent to a hydraulic conductivity range of between 4.1 and 17.2 m/d.

The hydraulic characteristics of the individual high-permeability zones of the two flow zones in the Lower Floridan aquifer at the Lake Okeechobee injection-well site can be estimated using the following mathematical procedure:

$$Q_T = Q_1 + Q_2 + Q_3 + Q_4 \quad (1)$$

where:

Q_T is the total flow rate through the well, and

Q_i (i = 1,2,3,4) represents the flow components from the different aquifer high-permeability zones.

For radial flow through each flow zone, Darcy's law can be expressed as:

$$Q_i = 2\pi r T_i \frac{dh_i}{dr} \quad (2)$$

where:

r is the radial distance from the pumping well,

T_i is the transmissivity in the i-th high-permeability zone,

dh_i is the head change in the i-th high-permeability zone, and

dr is the change in distance from the pumping well.

Assuming a very small difference in head gradient among the high-permeability zones, $dh_i/dr = dh/dr$, and uniform head distribution in the wellbore, equation *(2)* becomes:

$$Q_T = 2\pi r\left(T_1 + T_2 + T_3 + T_4\right)\frac{dh}{dr} = 2\pi r T \frac{dh}{dr} \quad (3)$$

and:

$$T = T_1 + T_2 + T_3 + T_4 = K_1 b_1 + K_2 b_2 + K_3 b_3 + K_4 b_4 \quad (4)$$

Based on the previous assumptions, $Q_i/Q_T = T_i/T$ and $T_i = K_i b_i$. The average hydraulic conductivity of each high-permeability interval i can be estimated if the thicknesses (b_i) of the high-permeability zones are known. The hydraulic conductivity values K_i for the four high-permeability zones, given in table 1, were estimated using the flow terms Q expressed as a percentage (where Q_T = 100), assuming that all flow comes from the four high-permeability zones, and using the transmissivity value estimated at the injection well (71,000 m^2/d).

Aquifer matrix permeability (k_i, intrinsic permeability) values, given in table 1, were computed using:

$$k_i = \frac{\mu K i}{\rho g} \quad (5)$$

where:

μ is the dynamic viscosity of the fluid [M/LT],

ρ is fluid density [M/L^3], and

g is the gravitational acceleration vector [L/T^2].

Subsurface Injection, Storage, and Recovery Concept

Subsurface injection, storage, and recovery of freshwater in brackish or saline aquifers is a water supply storage strategy that has received increased attention in recent years. The subsurface injection, storage, and recovery concept is suited for southern Florida where there is: (1) a surplus of freshwater during the wet season; and (2) a lack of suitable surface storage reservoirs because of the cost of land, limits of topography, and high rates of evapotranspiration and seepage losses. The suitability of a particular aquifer to store surface water is determined through subsurface injection, storage, and recovery tests from which the recovery efficiency (ability of the well/aquifer system to retrieve some fraction of the injected water) is determined.

The success of subsurface injection, storage, and recovery of freshwater is measured by the recovery efficiency. The recovery efficiency is defined as the volume of mixed injected and native aquifer waters recovered that meets a prescribed chemical standard, expressed as a percentage of the volume of water initially injected (Meyer, 1989). Most recent studies of subsurface injection, storage, and recovery have assumed the recommended level of 250 mg/L (milligrams per liter) for chloride concentration as the standard (Florida Department of Environmental Protection, 1993). However, in this study a limit of 1,385 mg/L of chloride and a limit of specific conductance of 5,000 µS/cm (microsiemens per centimeter) were established because the potential use (agricultural irrigation) of the recovered water tolerates this salinity level. This salinity level is the upper limit that can be tolerated by most crop types.

Merritt and others (1983) and Merritt (1985) describe a number of physical mechanisms that control the recoverability of freshwater injected into the Floridan aquifer system. They determined that buoyancy stratification, mixing due to hydrodynamic dispersion, and downgradient displacement of the injected freshwater with the native water were the three dominant processes that affected the recovery efficiency.

Buoyancy stratification is the process in which the lighter freshwater rises through the aquifer while moving outward from the injection well and overrides the denser, native saltwater or brackish water. Buoyancy stratification can be very significant especially during long storage periods. During recovery, native saltwater in the lower part of the injection zone is drawn into the well, whereas freshwater remains in the upper part of the zone. Buoyancy stratification is controlled by the density contrast between native and injected waters, permeability of the injection zone, and thickness of the injection zone (Merritt, 1985). Studies by Merritt and others (1983) and Merritt (1985) indicate that thin aquifers of moderate permeability are less affected by buoyancy stratification, and therefore, best suited for subsurface injection, storage, and recovery of freshwater. Confinement of the injection zone by low-permeability hydrogeologic units can also aid in limiting the upward movement of freshwater.

Hydrodynamic dispersion describes the mixing of solutes due to molecular diffusion and mechanical dispersion. Molecular diffusion is the process that describes the movement of solute particles from areas of high solute concentration to areas of low solute concentration. The effect of molecular diffusion is independent of the fluid velocity. Mechanical dispersion is caused by mixing of solutes due to variations in fluid velocities at the microscopic scale. Enhanced mechanical dispersion or macrodispersion is caused by velocity variations resulting from local differences in hydraulic conductivity. At the relatively large velocities during injection and recovery, the effects due to mechanical dispersion are generally far greater than those due to molecular diffusion. During long-term storage, however, molecular diffusion may become the dominant mixing process.

A transition zone is created during the mixing of the native and injected waters. The extent of the transition zone depends on the rate of injection, length of injection period, and the difference in solute concentration between the native and injected waters. Because velocities are higher near the well, most of the mixing occurs at the start of the injection process. As injection continues, the transition zone moves outward at continually decreasing velocities, leading to decreasing dispersive mixing at the interface between the native and injected water.

The effect of downgradient displacement of the injected freshwater body on recovery efficiency depends on the length of the injection-recovery cycle and the regional ground-water flow velocities. For subsurface injection, storage, and recovery cycles of relatively short duration (with respect to the size (scale) of the aquifer system), this effect can be considered negligible because the local hydraulic gradient due to injection is much greater than the regional gradient.

Clogging of the aquifer around the injection wellbore is another factor that can affect the recovery efficiency. Clogging can be caused by bacterial growth, suspended sediments in the injected water, and chemical precipitation of solutes due to reactions between the injected water and the aquifer matrix or native water. At the Lake Okeechobee well facilities (fig. 1), the injection well is open hole from 377 to 509 m below sea level and the aquifer is characterized as cavernous. None of the aforementioned clogging problems are likely to occur for such a well-aquifer system. However, geochemical models can be used to predict the reactions that would most likely occur during rock-water interaction and mixing of injected and native waters.

Acknowledgments

The authors wish to thank the personnel of the South Florida Water Management District for their extraordinary effort in coordinating the fieldwork. Special thanks to Keith Smith and Marty Braun of the Hydrogeology Division and Scott Burns formerly of the Hydrogeology Division.

TESTS OF SUBSURFACE INJECTION, STORAGE, AND RECOVERY OF FRESHWATER

A series of freshwater subsurface injection, storage, and recovery tests were conducted at the Lake Okeechobee injection-well site to assess the recoverability of injected canal water from the Lower Floridan aquifer. The injected water was withdrawn from the L-63N canal, which collects water from Taylor Creek and Nubbin Slough (fig. 1). The canal water is composed of runoff and local ground-water discharge from shallow infiltration. According to Quiñones-Aponte and Whitley (1996, in press), the injected canal water and the water in the Lower Floridan aquifer are of similar major inorganic composition.

The subsurface injection, storage, and recovery facilities have been previously described in this report and consist of an injection well that is 60.96 cm (centimeters) in diameter and a nest of two monitor wells, one shallow and one deep, located about 171 m from the injection well (fig. 1). The injection well is cased to a depth of 377 m below sea level and open hole to 509 m below sea level in the Lower Floridan aquifer. The shallow and deep monitor wells were used to observe water-quality changes due to mixing of the injected canal water and native aquifer water in the Lower Floridan aquifer. The shallow well is 15.2 cm in diameter and open to the middle semiconfining unit of the Floridan aquifer system from 292 to 318 m below sea level. The deep well completed in the Lower Floridan aquifer is 3.8 cm in diameter and is open to the aquifer from 379 to 539 m below sea level.

Background water-quality data were collected prior to the subsurface injection, storage, and recovery cycles. CH_2M Hill (1989) used a straddle packer to conduct hydraulic testing and collect water samples from four depth intervals (349 to 365 m, 383 to 403 m, 401 to 450 m, and 460 to 497 m below sea level). These depth intervals do not necessarily coincide with the high permeability zones included in table 1, but some may include the high-permeability zones. The data, presented in table 2, indicate that chloride, specific conductance, and total dissolved solids values were significantly different between zones and increased with depth. This suggests that there is some degree of semiconfinement among the high-permeability zones.

Initial testing was conducted by CH_2M Hill (1989) at the Lake Okeechobee injection-well site to: (1) estimate the maximum feasible injection rate, (2) determine if pretreatment by chlorination would be necessary to eliminate potential fecal coliforms in the injected water, and (3) evaluate the recoverability of the injected canal water. Results indicated that water can be injected into the Lower Floridan aquifer through the injection well at a rate from 18,925 to 37,850 m^3/d (cubic meters per day). Chlorination had little effect on coliform concentrations in the brackish environment of the Lower Floridan aquifer. CH_2M Hill (1989) further reported that water can be withdrawn from the well (under the natural and built-up artesian pressures of the aquifer) at a rate from 10,976.5 to 16,275.5 m^3/d. CH_2M Hill also indicated that the recoverability of the injected canal water could be enhanced by increasing the volume to be stored and/or backplugging the deeper saline zone of the aquifer that is open to the injection well (456 to 509 m below sea level). However, actual testing of this hypothesis was beyond the scope of the study (CH_2M Hill, 1989). CH_2M Hill (1989) indicated that density might affect the recovery efficiency. Most of their tests were affected by the relatively small volumes injected, about 94,600 to 344,185 m^3 (cubic meters), and the duration of the storage period (0 to 28 days). Such

Table 2. Background water-quality data for the canal water and native-aquifer water at the Lake Okeechobee injection-well site

[Data from CH_2M Hill (1989); straddle packer used to conduct tests in monitor well test hole]

Water type	Straddle packer test depth interval (meters below sea level)	Representative high-permeability zones (from table 1)	Chloride (milligrams per liter)	Field specific conductance (microsiemens per centimeter)	Total dissolved solids (milligrams per liter)	Static water-level altitude (meters, sea level)
Canal			290	1,140	729	
Native aquifer	349-365	Middle semiconfining unit	131	1,155	656	13.3
	383-403	1	1,800	7,850	4,000	12.4
	401-450	2	2,500	10,890	5,740	12.1
	460-497	3,4	2,920	12,763	6,710	11.9

conditions precluded recovery of meaningful quantities and impeded the interpretation of the test results in terms of the recovery efficiency. When the amount of injected water is small (relative to the size of the aquifer), the conditions represented by the data do not actually represent the aquifer, but the well/aquifer interface. CH_2M Hill (1989) could not make any projections or a conclusive assessment of the recovery efficiency potential because of the relatively small volume injected.

Four subsurface injection, storage, and recovery cycles were conducted for the present study, as was the case for the study by CH_2M Hill (1989). Cycle 1 consists of injection and recovery phases; cycles 2 and 3 consist of injection, storage, and recovery phases; and cycle 4 consists only of an injection phase. The injection, storage, and recovery phases are explained below:

- Injection: Phase in which canal water is injected through the well into the formation using a pump.
- Storage: Period in which the well is shut-in, and
- Recovery: Phase in which water is withdrawn from the aquifer (through the injection/recovery well) by natural artesian flow. A 35.6-cm diameter valve was open, discharging at rates ranging from 16,460 to 18,532 m^3/d. The water was discharged into a detention pond and later released into the L-63N canal (fig. 1).

The volumes of water injected ranged from 387,275 to 1,343,675 m^3 in the present study and ranged from 94,600 to 344,185 m^3 in the study by CH_2M Hill (1989). A preestablished water-quality limit (5,000 µS/cm of specific conductance, which is equivalent to a chloride concentration of 1,385 mg/L) was used to end the recovery cycle and determine the recoverability of water. Recovery was terminated when these water-quality criteria were met at the injection well. The results of the four injection, storage, and recovery cycles for the present study are discussed in the subsequent sections of this report.

Cycle 1

Cycle 1 consisted of injection and recovery phases. A preinjection phase was conducted for cycle 1, during which background water-quality conditions were established when specific conductance and chloride values were 10,400 µS/cm and 3,100 mg/L in the injection well, 7,930 µS/cm and 2,200 mg/L in the deep monitor well, and 1,280 µS/cm and 210 mg/L in the shallow monitor well. The amount of water discharged from the flowing well into the detention pond before reaching the background water-quality conditions was about 1,890 m^3. Corresponding constituents in water samples collected from the injection well and from the straddle packer test at an interval of between 383 and 403 m below sea level in the deep monitor well (table 2) were similar to background chloride and specific conductance values.

The injection phase of cycle 1 was conducted over a 35-day period in spring 1991 (April 17 to May 22), and the volume of water injected was 686,324 m^3. During this period, the injection rate ranged from 16,400 to 21,700 m^3/d and averaged 20,186 m^3/d (fig. 3A and table 3). The specific conductance and chloride values in the injected water were 709 µS/cm and 150 mg/L, respectively. All water samples were collected at the wellhead; the reason being that water

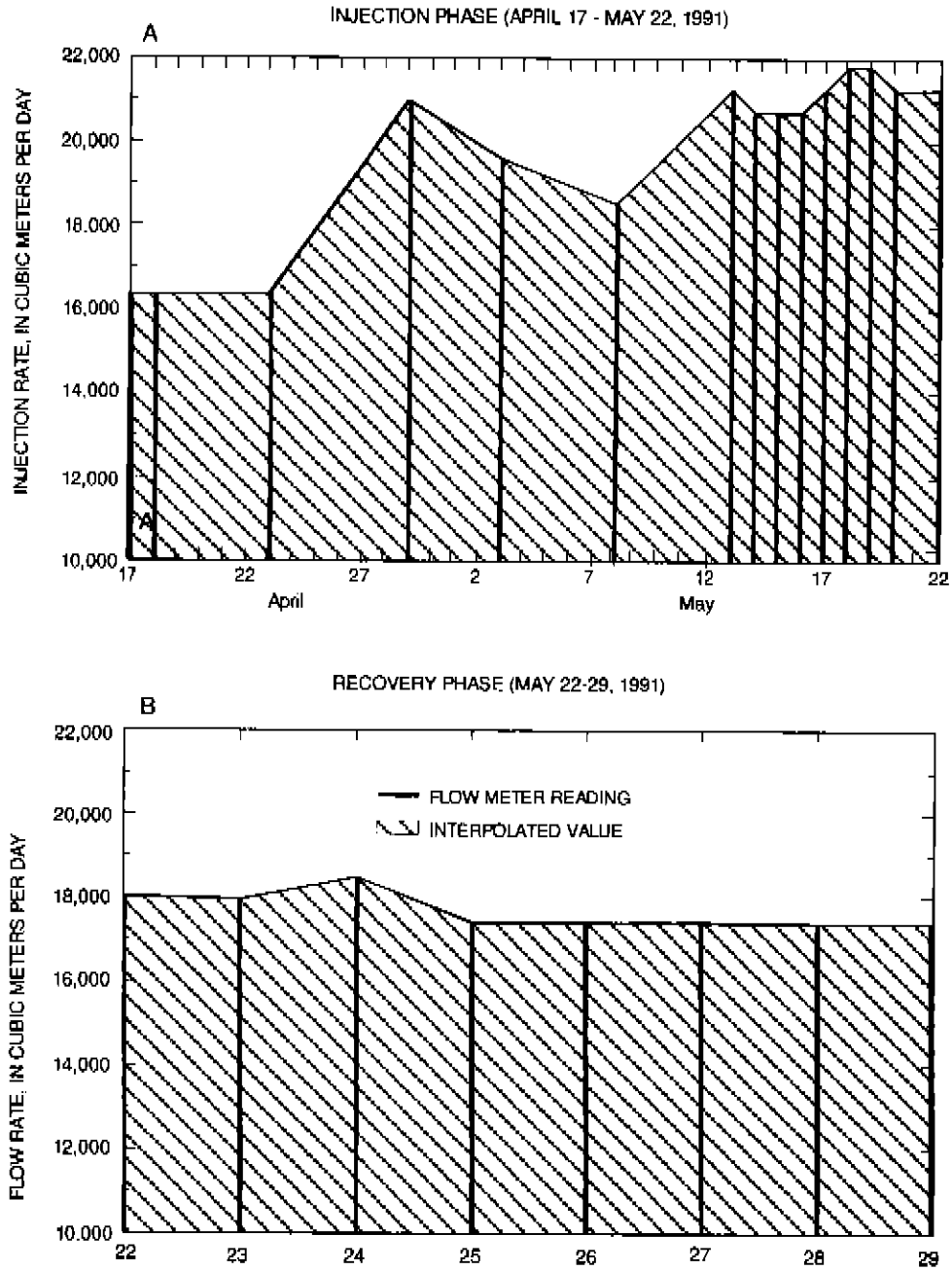

Figure 3. Rates of injection and recovery for cycle 1.

Table 3. Summary of results from subsurface injection, storage, and recovery cycles at the Lake Okeechobee injection-well site

Cycle number	Volume of water injected (cubic meters)	Volume of water recovered (cubic meters)	Storage period (days)	Average injection rate (cubic meters per day)	Average recovery rate (cubic meters per day)	Recovery efficiency (percent)
CH_2M Hill[1]	344,185		0	17,201	13,693	24
1	686,324	106,200	0	20,186	17,700	15
2	1,294,784	287,162	8	20,552	16,892	22
3	1,343,675	484,400	5	21,043	[2]17,300	36
4	387,275	--	--	14,549	--	--

[1]Data from CH_2M Hill (1989) test no. 4

[2]Estimated using flow-meter readings from cycles 1 and 2.

levels in the injection, deep, and shallow monitor wells rise above land surface due to the artesian condition of the respective aquifers.

The recovery phase was conducted over a 7-day period (May 22-29, 1991) when the preestablished water-quality limit (5,000 µS/cm of specific conductance, which is equivalent to a chloride concentration of 1,385 mg/L) was reached at the injection well. Chloride concentrations in the injection well (and the shallow and deep monitor wells) for the injection and recovery phases of cycle 1 are shown in figure 4. During the recovery phase, an average flow rate of about 17,700 m^3/d was maintained (fig. 3B and table 3). The volume of water recovered prior to achieving the preestablished chloride concentration limit (fig. 4B) was 106,200 m^3, and the estimated recovery efficiency was about 15 percent (table 3).

Cycle 2

Cycle 2 consisted of injection, storage, and recovery phases. Background water-quality conditions were not preestablished for this cycle. The buffer zone, which was created by the mixing of native aquifer water and residual water injected during cycle 1, served as reference conditions for cycle 2. This procedure is described in the literature as a "successive cycle" (Merritt, 1985). Preinjection sampling indicated that specific conductances and chloride concentrations were 4,220 µS/cm and 1,100 mg/L in the injection well, 2,020 µS/cm and 480 mg/L in the deep monitor well, and 959 µS/cm and 140 mg/L in the shallow monitor well.

The injection phase of cycle 2 was conducted over a 63-day period in summer 1991 (June 24 to August 26), and the volume of water injected was 1,294,784 m^3. During this period, the injection rate ranged from 19,077 to 21,800 m^3/d and averaged 20,552 m^3/d (fig. 5A and table 3).

A storage period of about 8 days (August 26 to September 3, 1991) was allowed before the beginning of the recovery phase of cycle 2. The recovery phase was conducted over a 17-day period (September 3-20, 1991) prior to achieving the preestablished water-quality limit (5,000 µS/cm of specific conductance which is equivalent to a chloride concentration of 1,385 mg/L). Chloride concentrations in the injection well (and the shallow and deep monitor wells) for the injection and recovery phases of cycle 2 are shown in figure 6. During the recovery phase, the flow rate ranged from 16,460 to 17,545 m^3/d and averaged 16,892 m^3/d (fig. 5B and table 3). The volume of water recovered prior to exceeding the preestablished chloride limit at the injection well (fig. 6B) was 287,162 m^3 and the estimated recovery efficiency was about 22 percent (table 3).

Cycle 3

Cycle 3 also consisted of injection, storage, and recovery cycles. Background water-quality conditions were not preestablished for this cycle. The buffer zone water quality established by previous successive cycles of injection and recovery (described in the previous section) served as reference conditions for cycle 3. Preinjection sampling indicated that specific conductances and chloride concentrations were 5,020 µS/cm and

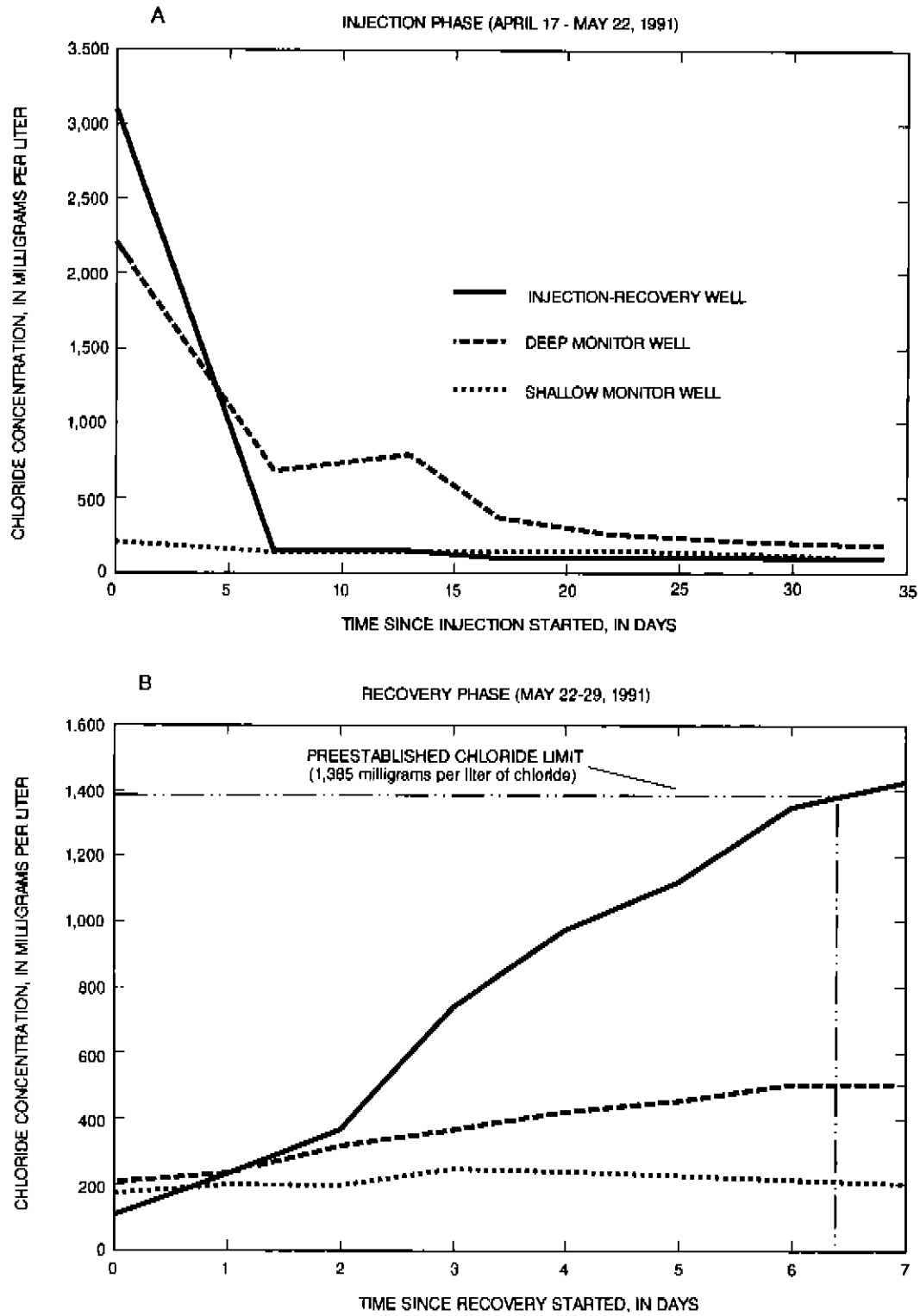

Figure 4. Chloride concentrations in the injection-recovery well and shallow and deep monitor wells during the injection and recovery phases of cycle 1.

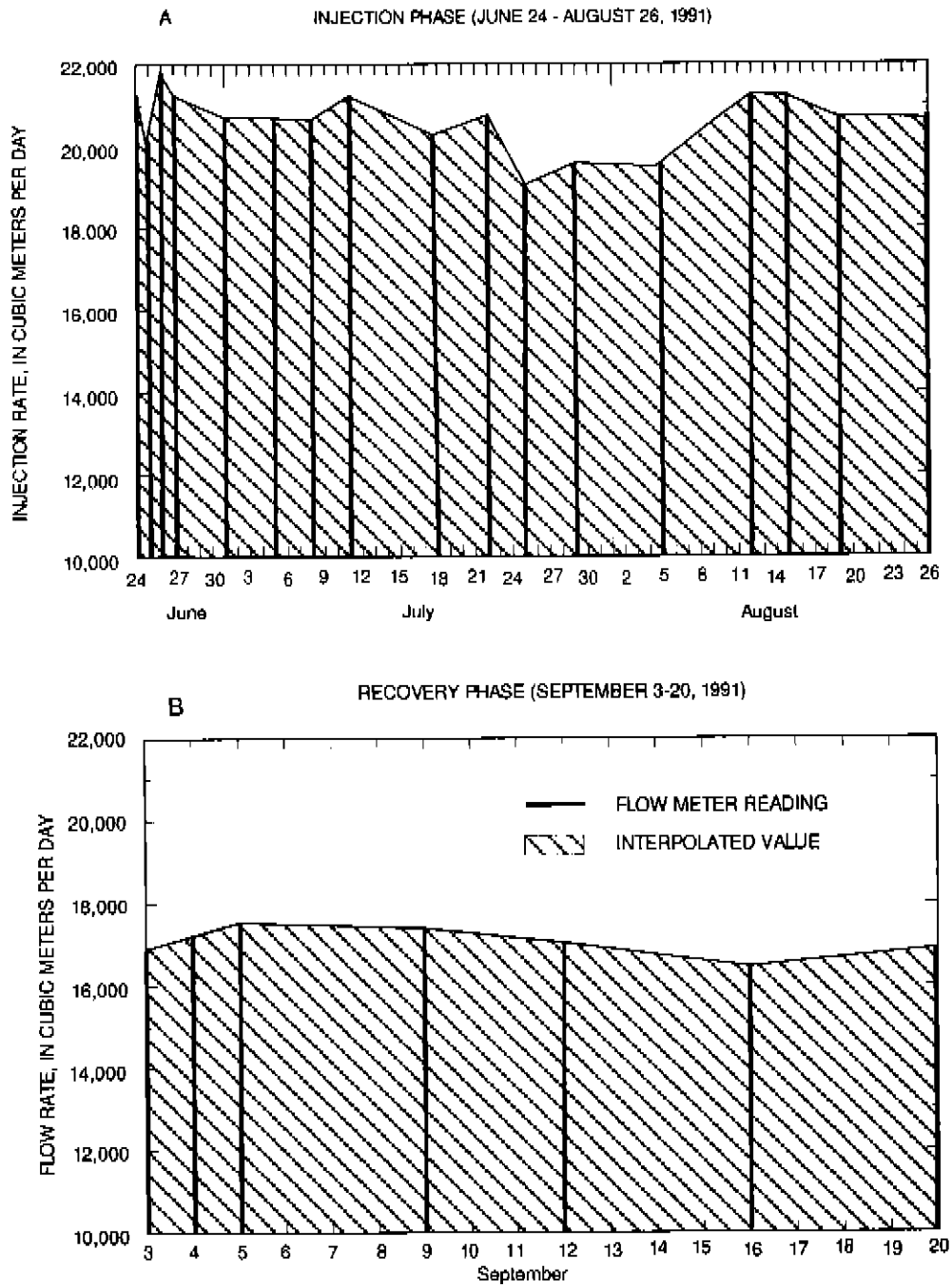

Figure 5. Rates of injection and recovery for cycle 2.

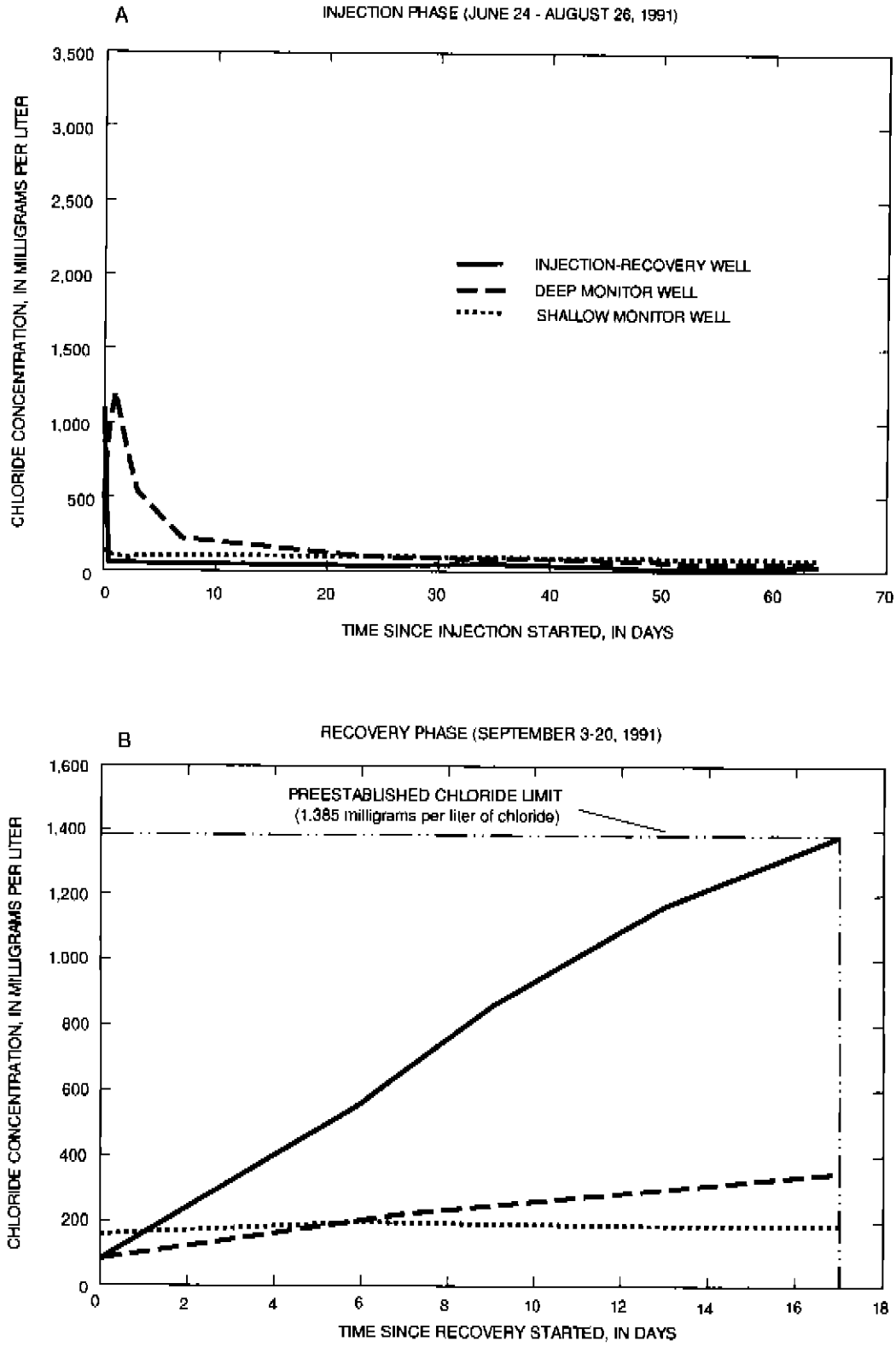

Figure 6. Chloride concentrations in the injection-recovery well and shallow and deep monitor wells during the injection and recovery phases of cycle 2.

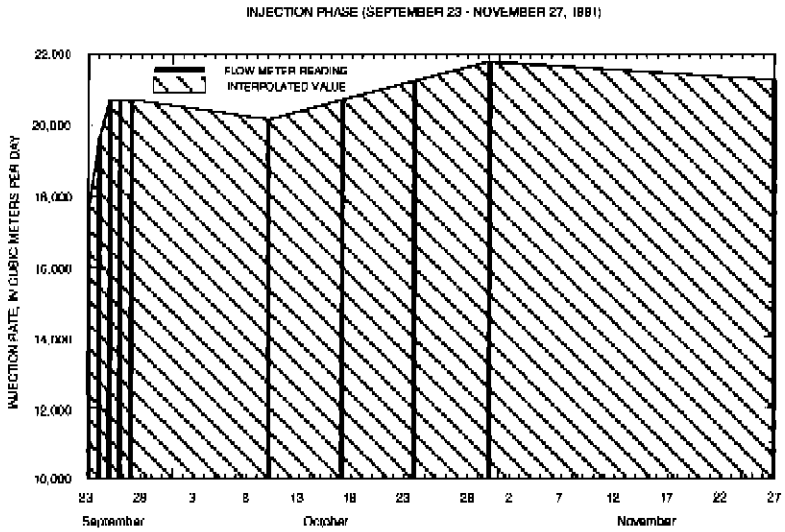

Figure 7. Rates of injection for cycle 3.

1,400 mg/L in the injection well, 1,410 µS/cm and 300 mg/L in the deep monitor well, and 929 µS/cm and 150 mg/L in the shallow monitor well.

The injection phase of cycle 3 was conducted over a 65-day period in autumn 1991 (September 23 to November 27), and the volume of water injected was 1,343,675 m^3. During this period, the injection rate ranged from 17,400 to 21,800 m^3/d and averaged 21,043 m^3/d (fig. 7 and table 3).

A storage period of about 5 days (November 27 to December 2, 1991) was allowed before the beginning of the recovery phase of cycle 3. The recovery phase was conducted over a 28-day period (December 2-30, 1991). Specific conductances and chloride concentrations at the end of the recovery period were about 4,700 µS/cm and 1,297 mg/L at the injection well. Chloride concentrations in the injection well (and the shallow and deep monitor wells) for the injection and recovery phases of cycle 3 are shown in figure 8. The recovery flow rate was not measured because of mechanical problems with the flow meter, but an average rate of 17,300 m^3/d was estimated using flowmeter readings from cycles 1 and 2. The specific conductance and chloride data were extrapolated through time because the chloride concentration limit of 1,385 mg/L was not reached at the end of the cycle. The volume of water recovered for the preestablished chloride limit (fig. 8B) was 484,400 m^3, and the estimated recovery efficiency was about 36 percent (table 3).

Cycle 4

Cycle 4 was used to define the dynamics of the aquifer system during the injection phase. Before injection, the valve at the wellhead was opened and water began flowing under natural artesian conditions. This backflow phase was conducted in an attempt to reestablish background water-quality conditions. Natural artesian flow was maintained for 161 days (January 27 to July 6, 1992). The natural artesian flow rate decreased with time during the test from more than 16,000 m^3/d to about 6,500 m^3/d. This may be an indication of pressure buildup in the aquifer during the injection phase. After 161 days of natural artesian flow, background water-quality conditions had not yet been reestablished at the injection and deep and shallow monitoring wells (fig. 9). The attempt to reestablish background water-quality conditions was abandoned because at least five additional months might have been required, and time constraints precluded continuation of the process (fig. 9). As a result, the reference water-quality conditions for cycle 4 consisted of lower chloride concentrations than those representing native aquifer water. The reference chloride concentrations (estimated from specific conductance readings) were about 2,700 mg/L at the injection well, 1,750 mg/L at the deep monitor well, and 240 mg/L at the shallow monitor well.

The injection phase of cycle 4 was conducted over a 26-day period in summer 1992 (July 8 to August 3), and the volume of water injected was 387,275 m^3.

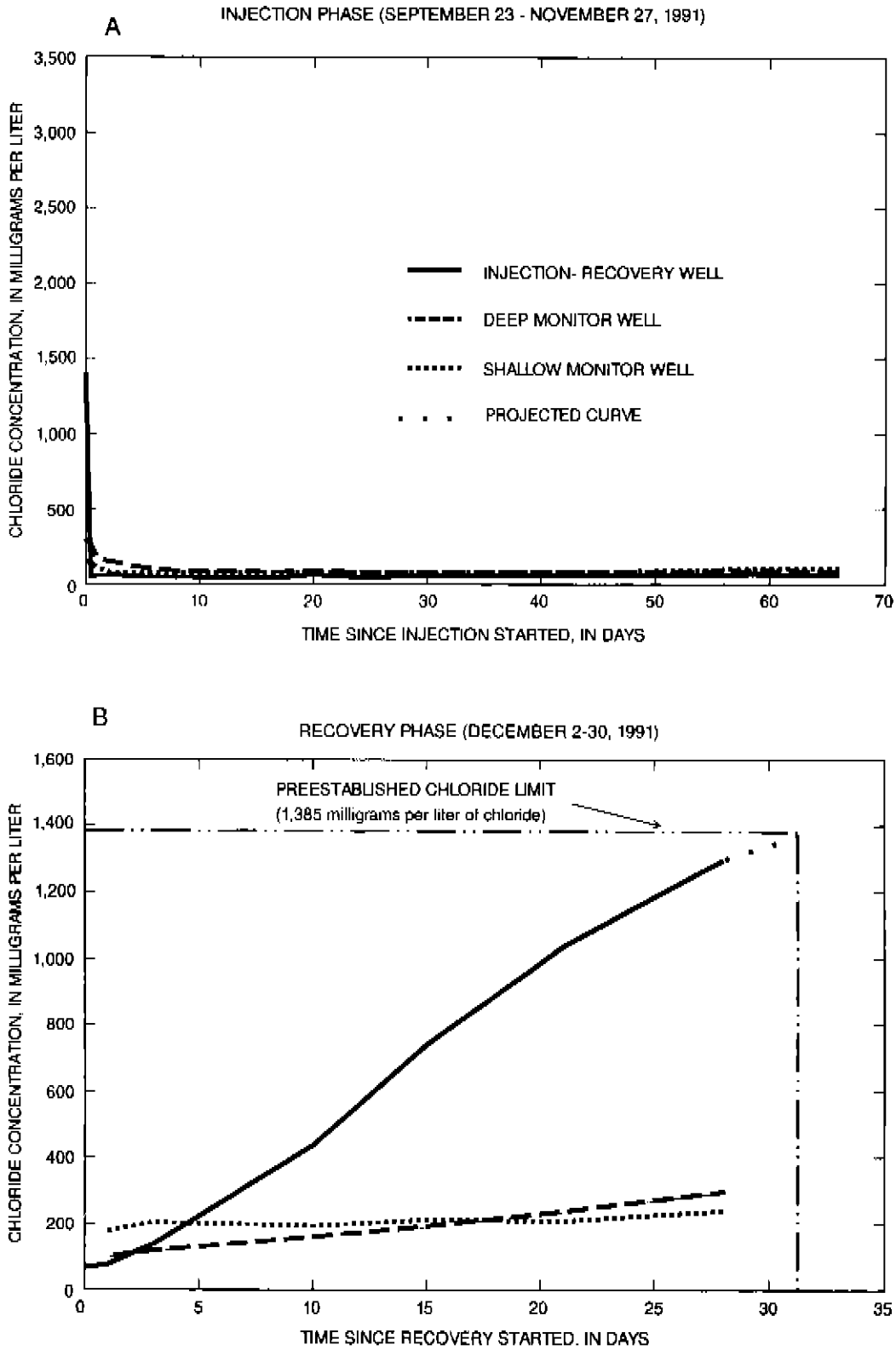

Figure 8. Chloride concentrations in the injection-recovery well and shallow and deep monitor wells during the injection and recovery phases of cycle 3.

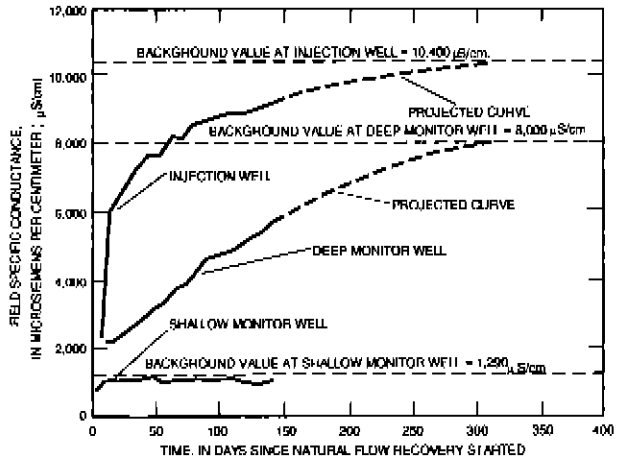

Figure 9. Specific conductance at the injection, deep monitor, and shallow monitor wells during the natural flow recovery period for reestablishing background water-quality conditions.

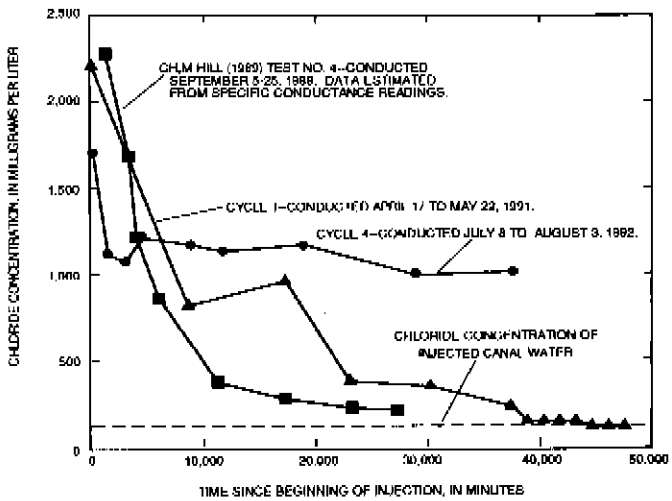

Figure 10. Chloride concentration breakthrough curves at the deep monitor well for the injection phase of cycles 1 and 4 from the present study and test no. 4 from a previous study.

An average injection rate of 14,549 m^3/d was maintained during this period (table 3). A storage period and a recovery phase were not conducted for cycle 4 due to the nature of the test.

Chloride concentration breakthrough curves were developed for the injection phase of cycles 1 and 4 (at the deep monitor well) from the present study data and test no. 4 from previous study data (CH_2M Hill, 1989). A comparison of the curves (fig. 10) reflects unexpected differences, especially considering that all three tests were conducted under similar background conditions. For example, it is expected that the chloride concentration curve reach an asymptote at a chloride concentration equal to that representative of canal water. Although it could be expected that the asymptote was reached at different times, for a conservative ion such as chloride, the asymptote should reach the same canal-water chloride concentration (chloride concentration of the injected water, approximately 120 mg/L). Several explanations of the hydrogeologic and hydraulic conditions at the injection well that may help explain this unexpected behavior are provided below.

1. Background chloride concentrations increased significantly with depth in the four high-permeability, relatively independent zones of the Lower Floridan aquifer. Chloride concentrations were 1,800 mg/L from 389 to 398 m below sea level (high-permeability zone 1),

2,500 mg/L from 419 to 424 m below sea level (high-permeability zone 2), 2,900 mg/L from 456 to 462 m below sea level (high-permeability zone 3), and 2,900 mg/L from 472 to 476 m below sea level (high permeability zone 4). These differences in background concentrations may have contributed to the anomalous patterns of the breakthrough curves (fig. 10).

2. Water-level altitudes, representative of the high permeability zones, were estimated from measurements using a straddle packer (CH_2M Hill, 1989) (table 2) and indicated a hydraulic gradient from the upper to the lower high-permeability zones. These data suggest that water from the upper high-permeability zone (1,800 mg/L of chloride concentration) might be flowing through the wellbore into the lower high-permeability zones (2,920 mg/L of chloride concentration). Hence, a mixing of the waters from the different high-permeability zones would occur, and the chloride concentration at which the asymptote of the breakthrough curve is reached would change (affected by the degree of mixing between the waters from the different zones).
3. The fact that the average injection rate for cycle 4 (14,549 m^3/d) was less than the natural artesian discharge rate (16,000 to 17,000 m^3/d) may have produced a greater degree of mixing at the deep monitor well (fig. 11). Figure 11A shows that if the injection rate (QINJECTED) were equal to or greater than the natural artesian flow (QNATURAL), all four high-permeability zones would transmit the injected water to the deep monitor well, and therefore, the chloride concentration value observed at the monitor well would be similar to that of the injected water. However, if QINJECTED were less than QNATURAL, the head differential might not be transmitted through the entire open wellbore, and injected water would probably flow only through the upper high-permeability zones (fig. 11B). As a result, chloride concentration values observed at the deep monitor well would represent a mix of water from the different high-permeability zones (fig. 11B), and therefore, would be higher than the concentration of the injected water.

ANALYSIS AND SUMMARY OF TEST CYCLES

Four subsurface injection, storage, and recovery cycles were conducted at the Lake Okeechobee injection-well site. Cycle 1 included injection and recovery phases; cycles 2 and 3 included injection, storage, and recovery phases; and cycle 4 included only an injection phase. The injection phases of each cycle were conducted over selected time periods in 1991 and 1992, and the volumes of water injected ranged from 387,275 to 1,343,675 m^3. The injection rate for cycles 1, 2, and 3 was similar and averaged about 20,600 m^3/d. The injection rate for cycle 4 was 14,549 m^3/d.

The recovery phases of cycles 1, 2, and 3 were conducted during variable time periods in 1991 when the preestablished water-quality limit was achieved at the injection well. The preestablished water-quality limit (5,000 µS/cm of specific conductance, which is equivalent to 1,385 mg/L of chloride concentration) was achieved for cycles 1 and 2 and projected for cycle 3. The average recovery flow rate ranged from 16,892 to 17,700 m^3/d for the three cycles. The volume of water recovered prior to achieving the preestablished water-quality limit ranged from 106,200 to 484,400 m^3, and the resulting recovery efficiency ranged from 15 to 36 percent.

The variability of the injection and recovery rates is shown in figures 3, 5, and 7 and can be due to several factors. Three of these factors include measurement device error (flow meter), change in background pressure, and electrical power failure (for the case of injection).

A comparison of the recovery efficiency for cycles 1, 2, and 3 in this study and test no. 4 from a previous study (CH_2M Hill, 1989) has been made, and the results are shown in figure 12. The recovery efficiency for successive cycles 2 and 3 increased from 22 to 36 percent and is expected to continue increasing with additional cycles. Cycle 1 and test no. 4 were conducted under similar background conditions (background conditions equal to native-aquifer water conditions or no residual injected water from a previous test). The volume of water injected for cycle 1 was 686,324 m^3 and the volume injected for test no. 4 was 344,185 m^3. Results indicated that the recovery efficiency was 24 percent for test no. 4 and 15 percent for cycle 1, suggesting that the recovery efficiency decreases with increasing injected volumes of water for tests conducted with no residual injected water from previous tests (background conditions equal to native-aquifer water conditions). All of these results are in agreement with those from previous studies by Tibbals and Frazee (1976) and Quiñones-Aponte and others (1989).

Cycle 4 was conducted in 1992 to define the dynamics of the aquifer system during the injection phase. A comparison of chloride concentration breakthrough curves at the deep monitor well (about 171 m from the injection well) for cycles 1 and 4 and test no. 4 reflects unexpected differences, especially considering that all three tests apparently were conducted under similar background conditions. One major difference was that the asymptote, expected to be reached at

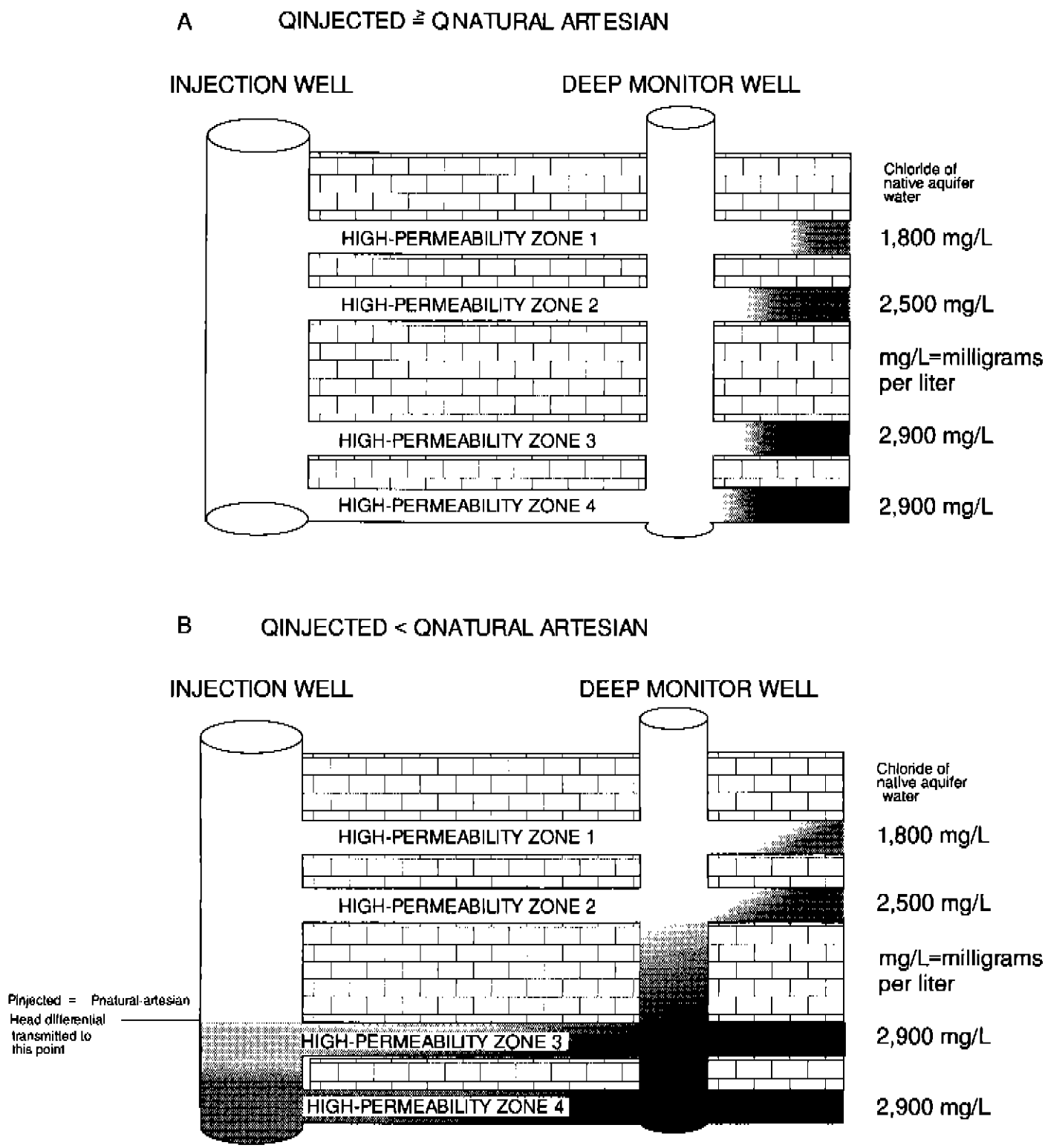

Figure 11. The injection process for two injection/recovery rate ratios: (A) QINJECTION/QNATURAL ARTESIAN is greater than or equal to 1.0, and (B) QINJECTION/QNATURAL ARTESIAN is less than 1.0.

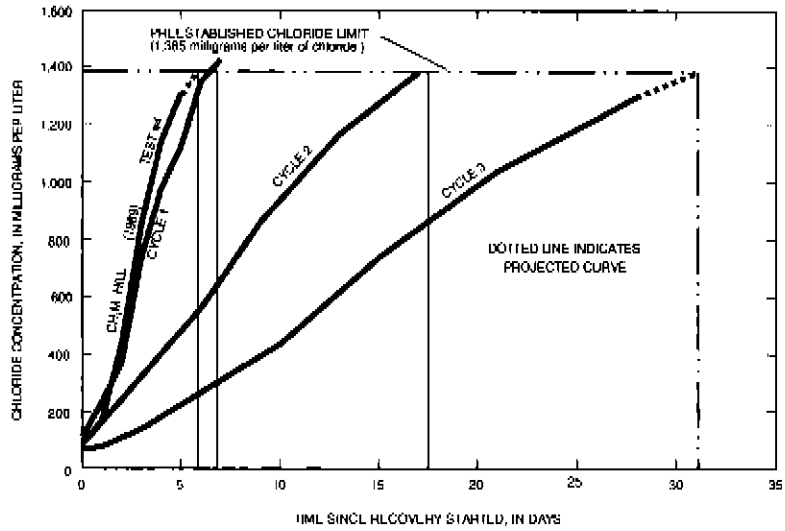

Figure 12. Chloride concentrations in the injection well during the recovery phase of cycles 1, 2, and 3 from the present study and test no. 4 from a previous study.

concentration levels equivalent or close to the injected water concentration, was instead reached at higher concentration levels.

Analysis of chloride concentrations in water at the injection-recovery well and at the deep monitor well (figs. 4, 6, and 8) indicates that flow through the Lower Floridan aquifer is not representative of a simple uniform-isotropic outflow of freshwater in a confined aquifer followed by a similar type of backflow. For the simple freshwater case of uniform-isotropic outflow and backflow within a porous media, changes in chloride concentration in water at the monitor well during recovery would precede changes in chloride concentration at the injection-recovery well. At some time during recovery, conditions at the monitoring well would return to background levels of chloride concentration because the bubble of injected water would clear the monitor well location while some freshwater still remained around the injection-recovery well. However, chloride concentrations returned to background levels at the injection-recovery well prior to achieving background conditions at the deep monitor well (figs. 4, 6, and 8). This suggests that the aquifer system is not characterized by a simple uniform-isotropic type flow, but instead responds as a conduit or cavernous type flow system. This hypothesis is illustrated by figure 11 and supports the corresponding discussion of cases where QINJECTED is less than QNATURAL. Figures 4, 6, and 8 also show that there were no significant changes in chloride concentration in water recovered from the shallow monitor well during the study, indicating that the injected freshwater did not reach this location vertically.

At the beginning of the recovery phase of cycle 1, chloride concentrations in water at the deep and shallow monitor wells were similar (fig. 4B). However, for cycles 2 and 3 (at the beginning of the tests), the chloride concentration in water at the deep monitor well was lower than in water at the shallow monitor well (figs. 6B and 8B). Additionally, the chloride concentration in water at the deep monitor well water at the beginning of cycles 2 and 3 was very similar to concentrations in water at the injection-recovery well (figs. 6B and 8B), indicating that injected water reached the deep monitor well during cycle 1 operations.

SIMULATION ANALYSIS OF SUBSURFACE INJECTION, STORAGE, AND RECOVERY OF FRESHWATER

The movement of solutes through porous media is controlled by both advection and hydrodynamic dispersion. Advective transport describes the movement of solute particles along the average direction of fluid flow at a rate equal to the mean pore-water velocity. Hydrodynamic dispersion describes the spread of solute particles along and transverse to the direction of average fluid flow in response to molecular diffusion and mechanical dispersion.

The following variable-density advective dispersive solute-transport equation was modified by

Quiñones-Aponte and Wexler (1995) for saturated flow and conservative solute species from a more general form presented by Voss (1984):

$$\frac{\partial (n\rho c)}{\partial t} = \nabla \bullet (n\rho v c) + \nabla \bullet \left[n\rho \left(D_d I + \underline{D}_m \right) \bullet \nabla c \right] + Q' c' \quad (6)$$

where:

n is the apparent porosity of the aquifer [dimensionless],

c is volumetric solute concentration in aquifer fluid [M/L^3],

t is time [T],

∇ is the gradient operator [1/L],

v is the average pore-water velocity [L/T],

D_d is the molecular diffusion coefficient [L^2/T],

I is the identity tensor (ones on diagonal, zero elsewhere),

$\underline{D}_m$ is the dispersion tensor [L^2/T],

Q' is the volumetric injection rate per unit area of aquifer [L/T], and

c' is volumetric solute concentration in the injected fluid [M/L^3].

In equation *(6)*, the term $Q' c'$ represents only sources of fluid. Withdrawals of fluid from the aquifer are not considered in equation *(6)* because the concentration of solute in the fluid being withdrawn, c', is identical to the solute concentration c in the aquifer.

The average pore-water velocity (v) needed to solve equation *(6)* can be determined by:

$$v = -\frac{q}{n} \quad (7)$$

where q is specific discharge (flow rate per unit cross-sectional area) [L/T].

The rate of ground-water flow (specific discharge) is represented by Darcy's law:

$$q = -k (\nabla p - \rho g z)/\mu \quad (8)$$

where:

k is the intrinsic permeability of the aquifer materials [L^2],

p is the fluid pressure [M/LT^2], and

z is the altitude above a reference datum [L].

The variable-density flow equation is developed using Darcy's law *(8)* and the principle of conservation of fluid mass:

$$\frac{\partial (n\rho)}{\partial t} = -\nabla \bullet (\rho q) \pm Q_p \quad (9)$$

where:

Q_p is the mass of fluid injected (+) or withdrawn (-) per unit time per unit volume of aquifer [M/L^{3}T].

A generalized digital model was constructed to simulate the subsurface injection, storage, and recovery of freshwater in the Lower Floridan aquifer at the Lake Okeechobee injection-well site. The model was constructed using a modified version of the Saturated-Unsaturated **TRA**nsport (SUTRA) code (Voss, 1984), which simulates variable-density advective-dispersive solute-transport and variable-density ground-water flow. This modified version of SUTRA for a regular rectangular grid, QSUTRA (Quiñones-Aponte and Wexler, 1995), reduces computer storage and time, allowing for more-detailed discretization. Like the original code (SUTRA), QSUTRA uses the Galerkin finite-element technique (Voss, 1984) to compute the solution of the ground-water flow and solute-transport equations. The ground-water flow equation *(9)* is solved using the Incomplete Cholesky-Conjugate Gradient method (Kuiper, 1987), and the solute-transport equation *(6)* is solved using the Line Successive Overrelaxation method (Young, 1954).

The simulations of freshwater injection, storage, and recovery in the Lower Floridan aquifer were made using the radial flow option of the QSUTRA code. Because of a lack of information on the spatial variability of the hydraulic and transport characteristics, several assumptions had to be made: (1) the effect of the background hydraulic gradient is negligible, (2) the aquifer is divided into vertically adjacent layers characterized in the model as homogeneous with respect to their hydraulic and transport characteristics, (3) the hydraulic and transport characteristics are homogeneous along the radial direction of flow, and (4) the aquifer characteristics are isotropic along the horizontal (radial) direction.

Model Concept and Construction

The conceptual model represents a generalized version of the Lower Floridan aquifer at the Lake Okeechobee injection-well site (fig. 1). It was developed on the basis of data obtained from geophysical logs, straddle packer tests, pumping tests, and injection tests during a previous study (CH_2M Hill, 1989). According to the data by CH_2M Hill (1989) and several

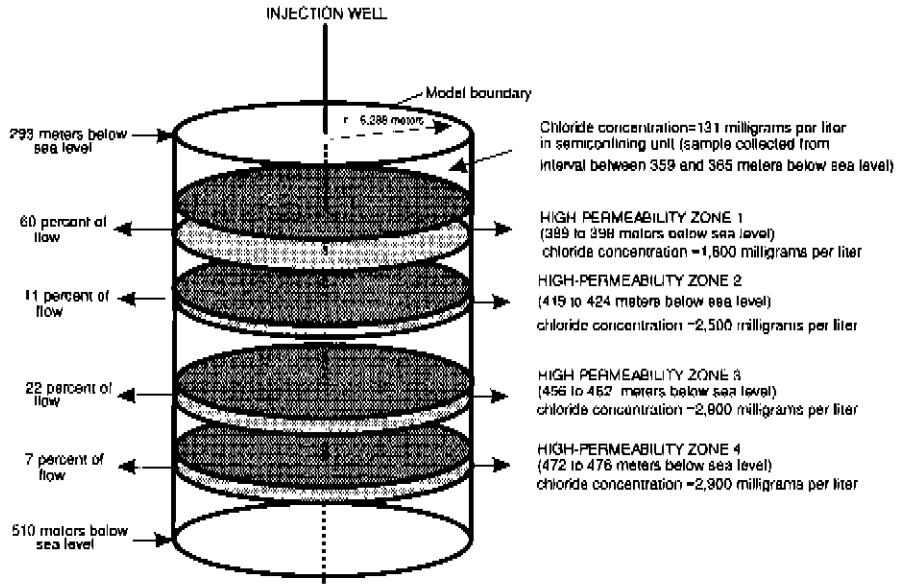

Figure 13. Generalized conceptual model of the Lower Floridan aquifer at the Lake Okeechobee injection-well site.

assumptions described previously, a generalized representation of the aquifer conditions at the site can be produced using a cylindrical coordinate system. This representative system can be justified for the case of injection or pumping from a single well where regional hydraulic gradients are small and aquifer hydraulic and transport characteristics are isotropic.

As previously discussed, the Lower Floridan aquifer can be visualized as containing four relatively independent high-permeability flow zones: high-permeability zone 1 (389 to 398 m below sea level), high-permeability zone 2 (419 to 424 m below sea level), high-permeability zone 3 (456 to 462 m below sea level), and high-permeability zone 4 (472 to 476 m below sea level). The high-permeability zones are characterized by fracture or cavernous type flow and are partly isolated from each other by hydrogeologic units of relatively low hydraulic characteristics. Sixty percent of the flow travels along high-permeability zone 1, 11 percent travels along high-permeability zone 2, 22 percent travels along high-permeability zone 3, and 7 percent travels along high-permeability zone 4 (fig. 13 and table 1). A very small percentage of the flow is transported as diffuse flow throughout the semiconfining units that are present between the high-permeability zones.

Water samples collected using a straddle packer (CH_2M Hill, 1989) indicated large differences in total dissolved solids, chloride concentrations, and water level altitude between the representative high permeability zones (table 2). High-permeability zone 1 had a total dissolved solids concentration of about 4,000 mg/L, a chloride concentration of about 1,800 mg/L, and a water-level altitude of 12.4 m. High-permeability zone 2 had a total dissolved solids concentration of about 5,740 mg/L, a chloride concentration of about 2,500 mg/L, and a water-level altitude of 12.1 m. High-permeability zones 3 and 4 had a total dissolved solids concentration of about 6,710 mg/L, a chloride concentration of about 2,920 mg/L, and a water-level altitude of 11.9 m. Although the high-permeability zones are relatively close to each other, the differences in water-quality data and water-level altitude indicated some degree of confinement between the zones. Additionally, an analysis of a water sample collected from 349 to 365 m, which represents a segment of the middle semiconfining unit (fig. 2), indicated that the total dissolved solids concentration was 656 mg/L and the chloride concentration was 131 mg/L (table 2). This result suggests that the degree of hydraulic connection among the high-permeability zones is relatively small.

Grid Design

A cylindrical coordinate finite-element grid was constructed (fig. 14) to study the subsurface injection, storage, and recovery cycles in the Lower Floridan aquifer at the Lake Okeechobee injection-well site. The model grid represents a radial extension of 6,288 m out

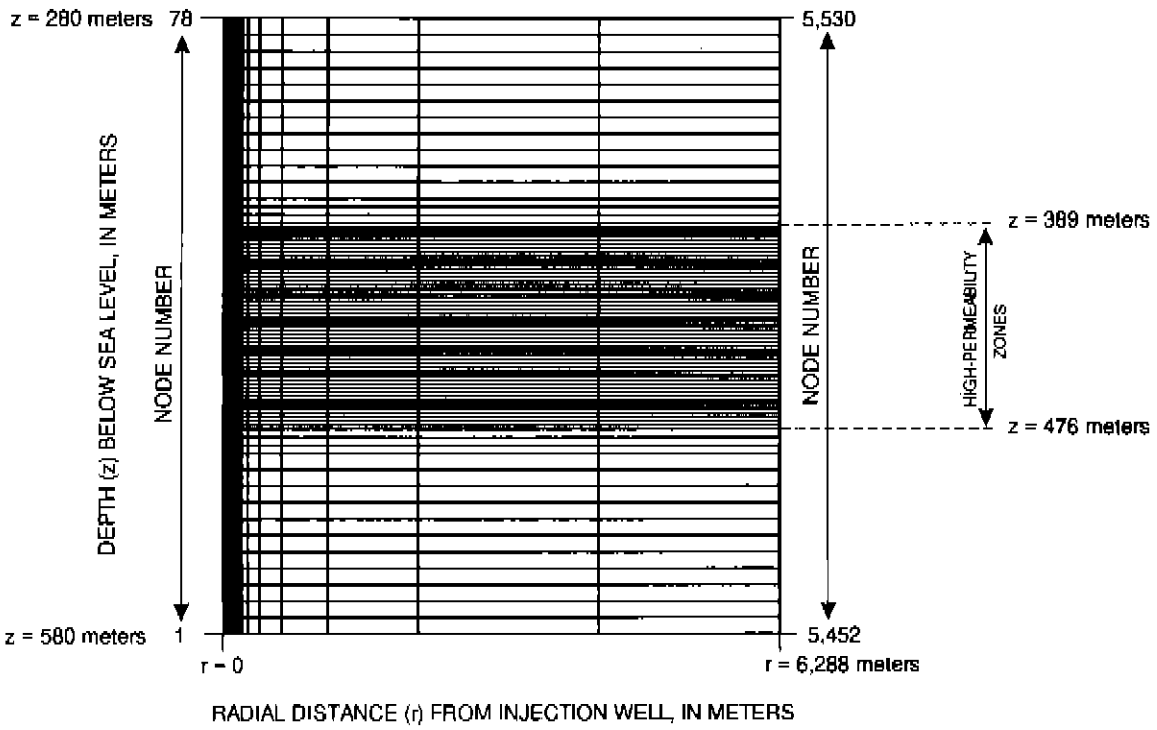

Figure 14. The cylindrical coordinate finite-element grid of the Lower Floridan aquifer at the injection-well site.

from the injection well into the aquifer. The grid is finer in the vicinity of the injection well to avoid errors associated with numerical dispersion (artificial dispersion due to inadequate discretization) and large differences between sides of a model-grid element. Elements represent a 2-m thickness and 2-m length near the well but vary elsewhere. Elements represent 4-m lengths at a distance of 100 m from the well, 8-m lengths at a distance of 120 m from the well, and lengths as much as 2,048 m beyond a distance of 160 m. Element thickness varied from 2 to 8 m, with 4-m thick elements providing a transition. Elements representing 8 m of aquifer thickness are used for the first 11 and last 11 rows of the model grid. Elements representing 2 m of aquifer thickness are used for 50 rows of the grid, corresponding to the aquifer interval that would be affected by injected canal water. Elements representing 4 m of aquifer thickness are used for 6 rows of the grid and correspond to a transition between the element rows representing thicknesses of 2 and 8 m (fig. 14).

Boundary and Initial Conditions

Boundary and initial conditions were determined for the generalized model of the Lower Floridan aquifer at the Lake Okeechobee injection-well site. Boundary conditions were set from $r = 0$ to $r = 6{,}288$ m at $z = 280$ m and $z = 580$ m below sea level, the limits of the finite-element grid (fig. 14). Specified pressure nodes were set at the top and bottom of the Lower Floridan aquifer with specified chloride concentration for any inflow across these boundaries (upper and lower limits of the modeled zone). Specified pressures were set equal to hydrostatic pressure ($P = h\rho g$). The chloride concentration was set equal to the concentration of the native water at these boundaries, which was obtained from in-situ samples. The boundary condition at the well ($r = 0$) was applied by specifying the mass flux equal to the injection rate. The flux was distributed among the boundary nodes along the length of the injection zone using an analysis from packer test data (fig. 13 and tables 1 and 2). The analysis showed that the flow distribution was 60, 11, 22, and 7 percent for high-permeability zones 1, 2, 3, and 4, respectively. The aquifer hydraulic characteristics (K and k) were determined in a similar manner using field determined transmissivity values and procedures described earlier in the report. A chloride concentration corresponding to the injected water during injection was specified at the well boundary ($r = 0$). A flux-average chloride concentration (weighted average concentration using flux as weighting factor) for water withdrawn during recovery was calculated using simulated chloride concentration values at boundary nodes representing the well (fig. 14, $r = 0$). The vertical lateral boundary (external boundary) was represented as a no-flow/

no-transport condition with the assumption that this boundary is sufficiently far away from the area of interest. At the upper and lower model limits, the constant pressure and concentration boundaries can be justified because of the distance from the injection source and the permeability gradients that exist throughout the 300-m thickness.

The initial pressures were assumed to be hydrostatic ($P = h\rho g$) and set equal to the equivalent freshwater head that corresponded to static conditions prior to injection. Initial chloride concentration was set equal to solute concentration in the native aquifer water at the different flow zones and boundaries (table 2). The fluid density ρ was assumed to depend only on solute concentration C and was calculated by the model based on initial solute concentrations and the following functional relation between density and solute concentration at each node:

$$\rho = \rho_i + (\rho_n - \rho_i)\left[(C - C_i)/(C_n - C_i)\right] \qquad (10)$$

where:

ρ_i is density of injected water [M/L^3],

ρ_n is density of native water [M/L^3],

C_i is solute concentration in injected water [M/L^3], and

C_n is solute concentration in native water [M/L^3].

Time Steps

To avoid numerical dispersion associated with a large time-step size, initial time-step sizes were set at or less than 100 seconds. The time-step size was increased during the injection phase so that the injected water front (neglecting dispersion) moved a constant distance with each successive time step. In the simulation of the mixing of two water bodies in a radial flow field, it is important to require that the time step, Δt, satisfies the condition:

$$\frac{v\ \Delta t}{2.0} \ll \alpha_L \qquad (11)$$

where α_L is the longitudinal dispersivity of the aquifer [L] (Kipp, 1987).

The time step must be of such size to permit the simulated movement of the injected water front inside a model element without an abrupt transition from one element to the next. For the radial coordinate system, water velocity increases as the water particles move closer to the well, and therefore, the time-step size must be increased during injection and decreased during recovery to meet the stability criterion established by equation *(11)*.

The final time-step size from the injection phase was used and maintained uniformly for the entire simulation of the storage period. During the recovery phase, the time-step size was gradually reduced from its maximum value as the injected water front moved closer to the well.

Calibration and Testing

The calibration and testing of the model was performed by changing the model variables within realistic limits, until a satisfactory comparison between the observed and simulated solute breakthrough data was obtained. Initial model variables were set according to data presented in tables 1 and 4. Other model constants are listed in table 5. A vertical anisotropy (k_H/k_V) ratio of 100:1 was assumed for the high-permeability zones and the semiconfining units that are present between the zones. For the semiconfining units, a horizontal intrinsic permeability value (k_H) of 1.53×10^{-11} m^2 (square meters) and a vertical intrinsic permeability value (k_V) of 1.53×10^{-13} m^2 were assigned. These values were derived using equation *(5)*, a k_H/k_V ratio of 100:1, and data from a CH_2M Hill (1989) straddle packer test in the middle semiconfining unit (349 to 365 m below sea level). The porosity for the semiconfining units between the high-permeability zones was assumed to be 0.15. The apparent effective porosity value listed in table 4 for the high-permeability zones was the result of calibration trials. Although conceptually this apparent effective porosity value (5 percent) seems to be too low for the high-permeability zones, it was the highest value (combined with the calibrated intrinsic permeabilities) to yield acceptable results in modeling the chloride concentration breakthrough curve at the deep monitor well.

Because the open intervals of the injection and monitor wells include more than one node, composite chloride concentration values representative of the wells were computed using simulated chloride concentrations at nodes representing the well. The computation was determined using a weighted average value (with permeability as a weighting factor) from nodes representing the open interval of the monitor wells and a flux-weighted average concentration value from nodes representing the injection well. Composite

Table 4. Aquifer characteristics used in the model of the Lower Floridan aquifer at the Lake Okeechobee injection-well site.

High-permeability zone	Depth interval (meters below sea level)	Horizontal permeability (square meters)	Vertical permeability (square meters)	Apparent effective porosity (percent)	Specific pressure storativity (kilograms per meter per second squared^{-1})	Longitudinal dispersivity (meters)	Transverse dispersivity (meters)
1	389-398	5.894×10^{-9}	5.894×10^{-11}	5	1.36×10^{-10}	1.0	0.1
2	419-424	1.945×10^{-9}	1.945×10^{-11}	5	1.36×10^{-10}	1.0	.1
3	456-462	3.242×10^{-9}	3.242×10^{-11}	5	1.36×10^{-10}	1.0	.1
4	472-476	1.547×10^{-9}	1.547×10^{-11}	5	1.36×10^{-10}	1.0	.1

Table 5. Fluid, solute, and rock matrix properties used in the simulations

[kg/m/s, kilograms per meter per second; kg/m^3, kilograms per cubic meter; m^2/s, square meters per second; (kg/m•sec^2)$^{-1}$, kilograms per meter per second squared^{-1}]

Property	Value
Dynamic viscosity of native water, in kg/m/s	0.001
Dynamic viscosity of injected water, in kg/m/s	0.00089
Density of native water, in kg/m^3	1,004.4
Density of injected water, in kg/m^3	1,000.1
Coefficient of molecular diffusion, in m^2/s	5.0×10^{-10}
Fluid compressibility, in (kg/m•sec^2)$^{-1}$	4.4×10^{-10}
Rock matrix compressibility, in (kg/m•sec^2)$^{-1}$	1.2×10^{-10}

chloride concentration values determined using the flux-weighted method are more accurate than composite concentration values from the permeability-weighted method. However, at the time of this study, the computer model (QSUTRA) does not provide for the computation of flux-weighted average concentrations at nodes representing an observation well.

Satisfactory comparisons of simulated to observed dimensionless chloride concentrations for the deep monitor well were obtained when using the model to simulate the injection and recovery phases of cycle 1 (fig. 15) using the parameters listed in table 4. Several attempts were made, changing the hydraulic and transport parameters by two or three orders of magnitude and changing the boundary conditions. Different combinations of no-flow and specified pressure boundary conditions were tested for the model limits. However, no acceptable comparison of simulated to observed dimensionless chloride concentrations for the injection well during the recovery phase of cycle 1 was obtained (fig. 16). A dimensionless version of chloride data obtained in the field (observed data) compared to dimensionless chloride data obtained from four calibration attempts (simulated data) for the injection well is shown in figure 16. The simulated data in figure 16 represent model results using the parameters in table 4 and represent the simulated values for different longitudinal and transverse dispersivities (α_L = 1.0 m and α_T = 0.1 m, α_L = 2.0 m and α_T = 2.0 m, α_L = 1.0 m and α_T = 1.0 m, and α_L = 1.0 m and α_T = 0.6 m).

Although many other calibration attempts were made, only the results for which the model input

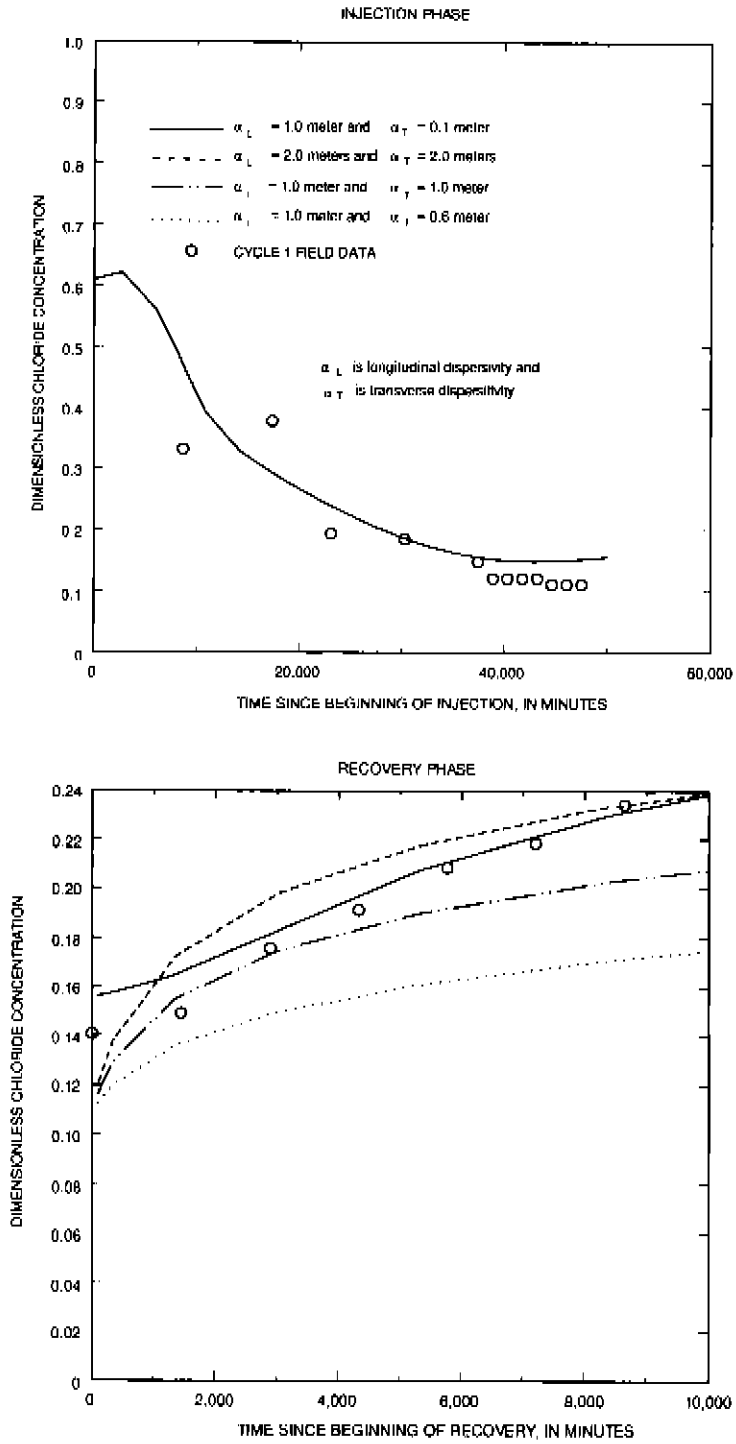

Figure 15. Observed and simulated dimensionless chloride concentration breakthrough curves at the deep monitor well during the injection and recovery phases of cycle 1.

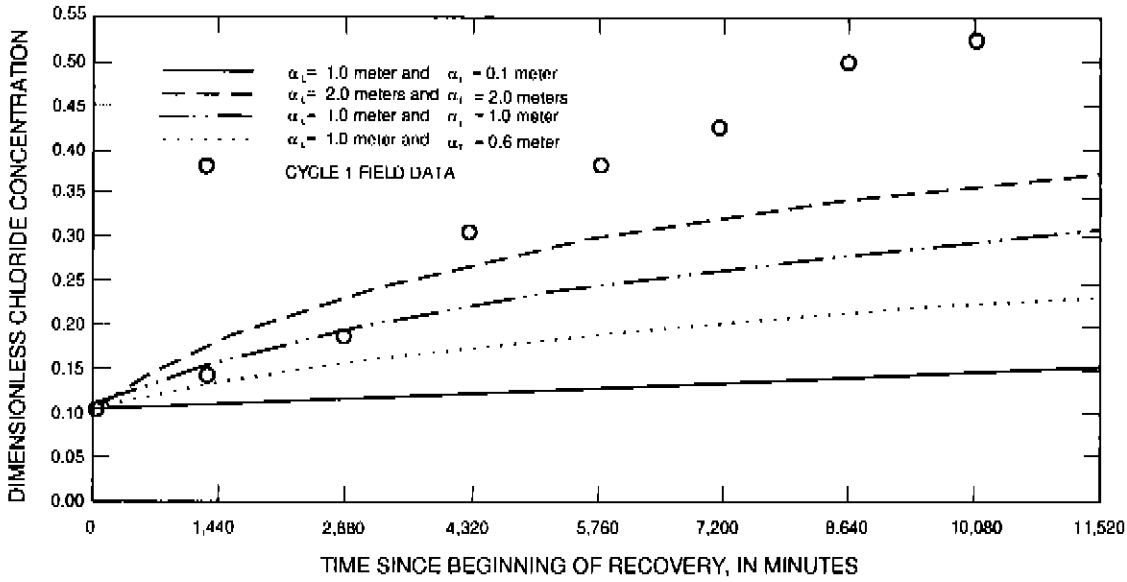

Figure 16. Observed and simulated dimensionless chloride concentrations in the injection well during the recovery phase of cycle 1.

variables were close to the parameters listed in table 4 are presented in this report. It was suspected that the cavernous/conduit nature of the Lower Floridan aquifer would allow for very high velocities (relative to typical ground-water velocities) to develop near the injection well. Such velocities would preclude an appropriate representation of flow and solute transport using the QSUTRA model, which is based on porous media assumptions. Porous media type models are based on Darcy's law which assumes a linear proportionality between specific discharge (discharge per unit measured of aquifer thickness) and hydraulic gradient. This proportionality is characteristic of laminar ground-water flow. The Reynolds number, defined below, is used to determine limits between laminar and turbulent flow regimes. For turbulent flow, the linear proportionality between specific discharge and hydraulic gradient is not valid. Where turbulent flow occurs, a porous media based flow model would compute hydraulic gradient distributions smaller than actual field gradients. Therefore, to test for the occurrence of turbulent flow, Reynolds numbers were estimated for different distances from the injection well using two different conceptual models, porous media and cavernous conceptual models. The Reynolds number (R_e) is defined as the ratio of inertial forces to viscous forces:

$$R_e = \frac{v\ d}{V} \qquad (12)$$

where:

d is a characteristic length (in this case, thickness of flow zone for cavernous conceptual system or $k^{1/2}$ [the square root of the intrinsic permeability] for the porous media conceptual system) [L], and

V is the fluid kinematic viscosity [L^2/T].

Reynolds numbers were only estimated for high-permeability zone 1 (9-m thick), which constituted 60 percent of the flow (fig. 13). The Reynolds numbers were estimated for two different conceptual systems in radial or cylindrical coordinates, a cavernous system and a porous media system (table 6). To estimate Reynolds numbers of actual field conditions at different distances from the injection source, it was necessary to determine or approximate the actual pore-water velocity at the different locations, the effective thickness of the flow zone (cavernous conceptual system) or intrinsic permeability (porous media conceptual system), and the fluid kinematic viscosity.

The actual radial ground-water flow velocity at a location from the injection source (the deep monitor well, located 171 m from the source) was determined from a chloride concentration breakthrough curve. This was accomplished by identifying the inflection point of the chloride concentration breakthrough curve, which usually coincides with the 50 percent concentration change from native to injected water. Data from test no. 4 by CH_2M Hill (1989) was used to estimate the pore-water velocity at the deep monitor well (fig. 17 and

Table 6. Sectional area, velocity, and Reynolds number estimated at different distances from the injection source

Radius (meters)	Area[1] (square meters)	Actual velocity (meters per second)	Reynolds number cavernous conceptual system (dimensionless)	Reynolds number porous media conceptual system (dimensionless)
0.1	0.0919	1.29961	13,539,167	112.3
.25	.2298	.51984	5,415,667	44.9
.5	.4596	.25992	2,707,833	22.4
1	.9191	.12996	1,353,917	11.2
2	1.84	.06498	676,958	5.6
4	3.67	.03249	338,479	2.8
6	5.51	.02166	225,653	1.8
8	7.35	.01624	169,240	1.4
10	9.19	.01300	135,392	1.1
12	11.02	.01083	112,826	.94
16	14.7	.00812	84,620	.70
20	18.4	.00650	67,696	.56
30	27.6	.00433	45,131	.37
40	36.8	.00325	33,848	.28
50	45.9	.00260	27,078	.22
100	91.9	.00130	13,539	.11
171	157	[2].00076	7,917	.066
200	184	.00065	6,770	.056
500	460	.00026	2,708	.022
1,000	919	.00013	1,354	.011
5,000	4,596	.00003	271	.0022

[1]The cavernous conceptual system is $2\pi rb \cdot correction\ factor$ and the porous media conceptual system is $2\pi rbn \cdot correction\ factor$ where r is the radial distance from the injection source, b is the thickness of the flow zone, and n is the apparent porosity of the aquifer (dimensionless). The correction factor was applied to adjust the thickness area of the flow zone in order to approximate actual field velocities. The correction factor was determined using the actual ground-water flow velocity estimated at the deep monitor well located 171 meters from the injection well.

[2]Actual field velocity estimated from a concentration breakthrough curve at the deep monitor well (fig. 17).

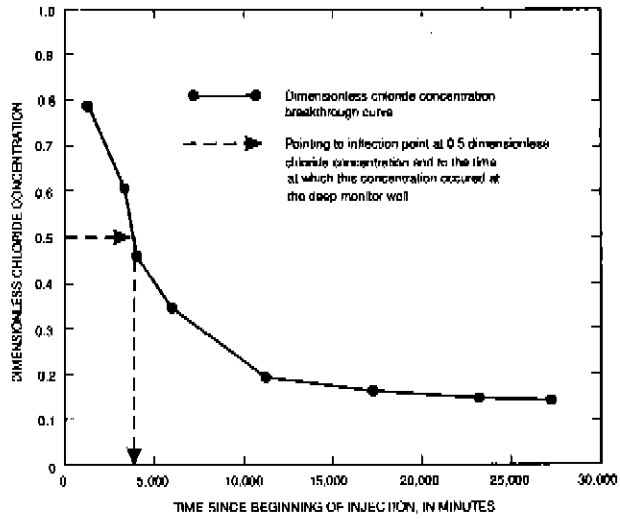

Figure 17. Dimensionless chloride concentration breakthrough curve of data from test no. 4. Test data from CH_2M Hill (1989).

table 3). These test data were selected for velocity determination because the subject test background concentration (native water concentration) was well established. This is important in determining the actual inflection point of the breakthrough curve (50 percent concentration change). The estimated pore-water velocity at the deep monitor well was 0.000760 m/s (meter per second). The area perpendicular to the flow for the case of radial flow is defined as $A = 2\pi rb$ where A is the area, r is the radial distance from the injection source, and b is the thickness of the flow zone. The effective area was first estimated at the location of the deep monitor well for which a velocity value was previously determined. The effective area was estimated by using the relation:

$$Q = v \cdot A_{eff} \cdot correction\ factor \qquad (13)$$

or:

$$A_{eff} = \frac{Q}{v \cdot correction\ factor} \qquad (14)$$

where Q is the flow through the flow zone. The correction factor was applied to the areas determined for different distance r to obtain an effective area (A_{eff}) for each location, and the effective area was used alone with flow rate to determine velocities at the different distances.

For the case of the porous media conceptual system, the square root of the intrinsic permeability of the high-permeability zone 1 (table 1) was used as the characteristic length as recommended by Bear (1979). Fluid kinematic viscosity in this zone was assumed as 8.639×10^{-7} m^2/s (square meters per second) at a water temperature of 26.7 degrees Celsius. For the case of the cavernous conceptual system, an effective thickness was determined using the same correction factors that were applied to the area to determine A_{eff} and used in equation *(12)* as the characteristic length.

For the porous media conceptual system, the Reynolds numbers were greater than 10 at distances less than 1.42 m from the injection well (fig. 18). This number (Reynolds number equal to 10) represents the upper limit of laminar porous media flow, which is the fundamental assumption for the application of Darcy's law to ground-water flow (Bear, 1979). At the deep monitor well located about 171 m from the injection well, the Reynolds number was about 0.08 which indicates laminar ground-water flow (porous media flow) at that location (fig. 18). The Reynolds number was about 100 at a distance of 0.1 m from the injection well (fig. 18). Thus, application of Darcy's law to ground-water flow is not valid at this distance nor is the transport solution, which is affected by the head gradient in the advection terms of the governing solute-transport equation. This may explain why the QSUTRA model produced good results for the deep monitor well, but was not able to produce acceptable results for the injection well. For the cavernous conceptual system, Reynolds numbers less than about 2,000 that are representative of laminar flow in circular tubes (Rouse,

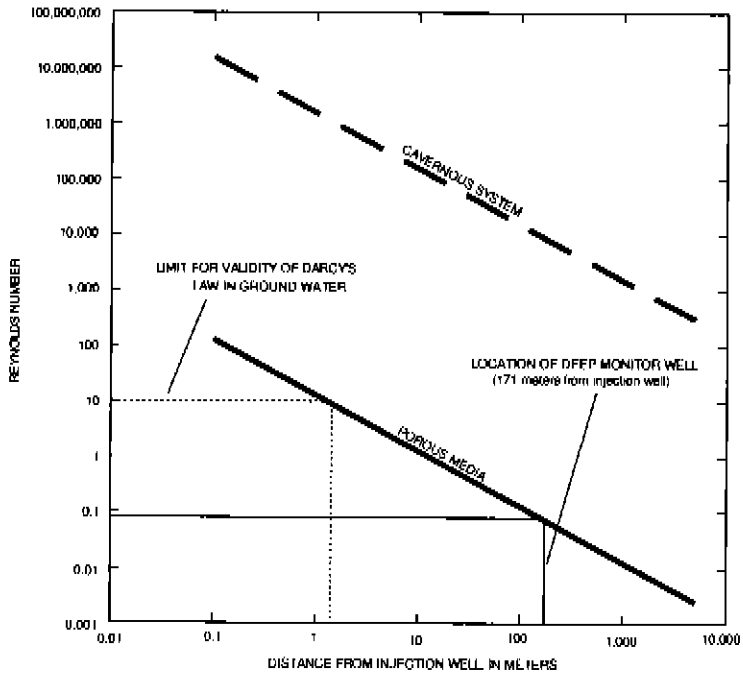

Figure 18. Reynolds number for a cavernous conceptual system and a porous media conceptual system as a function of distance from the injection well

1956, p. 174) were obtained at distances greater than 800 m (fig. 18). The Reynolds number was greater than 2,000 at distances less than 1,000 m from the injection well. This number represents the upper limit of laminar flow.

SUMMARY AND CONCLUSIONS

A series of freshwater subsurface injection, storage, and recovery tests were conducted at an injection-well site near Lake Okeechobee in Okeechobee County, Florida, to assess the recoverability of injected canal water from the Lower Floridan aquifer. Initial testing at the Lake Okeechobee injection-well site was previously conducted by a private consultant, and some of their results have been included as part of the U.S. Geological Survey study. At the study site, the Lower Floridan aquifer is characterized as having four local, relatively independent, high-permeability flow zones (389 to 398 m, 419 to 424 m, 456 to 462 m, and 472 to 476 m below sea level). The transmissivity of the aquifer at the injection well was estimated to be about 71,000 m^2/d from 377 to 509 m below sea level (equivalent to an average hydraulic conductivity of 540 m/d).

Four subsurface injection, storage, and recovery test cycles were conducted at the Lake Okeechobee injection-well site. Cycle 1 included injection and recovery phases; cycles 2 and 3 included injection, storage, and recovery phases; and cycle 4 included only an injection phase. The volumes of water injected ranged from 387,275 to 1,343,675 m^3 and the average injection rates ranged from 14,549 to 21,043 m^3/d for all the cycles. The volumes of water recovered, prior to achieving (or projecting) the preestablished water-quality limit (5,000 µS/cm of specific conductance, which is equivalent to about 1,385 mg/L of chloride concentration), ranged from 106,200 to 484,400 m^3 and the average recovery flow rates ranged from 16,892 to 17,700 m^3/d for cycles 1, 2, and 3. The recovery efficiency for successive cycles 2 and 3 increased from 22 to 36 percent and is expected to continue increasing with additional cycles. Cycle 1 and test no. 4 (from a previous study) were conducted under similar background conditions (background conditions equal to native-aquifer water conditions or no residual injected water from a previous test). The volumes of water injected were 686,324 m^3 for cycle 1 and 344,185 m^3 for test no. 4. The recovery efficiency was 24 percent for test no. 4 and 15 percent for cycle 1, indicating that the value decreases with increasing volumes of injected water. All these results are in agreement with those from previous studies.

Cycle 4 was conducted to define the dynamics of the aquifer system during the injection phase. A comparison of chloride concentration breakthrough curves at the deep monitor well (about 171 m from the injection well) for cycles 1 and 4 and test no. 4 reflects unexpected differences, especially considering that all three tests were conducted under similar background conditions. One major difference was that the concentration asymptote, expected to be reached at concentration levels equivalent or close to the injected water concentration, was instead reached at higher concentration levels. One factor that may explain the unexpected differences suggests that the ratio of injection to recovery rates could affect the chloride concentration breakthrough curves at the deep monitor well. For cases where the injection rate is smaller than the natural artesian flow rate, the head differential might not be transmitted to the deeper high-permeability zones. The injected water would probably reach the deep monitor well only through the upper high-permeability zones, and the chloride concentration values observed at this well would represent a mix of water from the different upper and lower high-permeability zones. Hence, the asymptote would be reached at a higher chloride concentration level in cases where the injection rate is smaller than the natural artesian flow rate.

A generalized digital model was constructed to simulate the subsurface injection, storage, and recovery of freshwater in the Lower Floridan aquifer at the Lake Okeechobee study site. The model was constructed using a modified version of the SUTRA code (QSUTRA). QSUTRA uses the Incomplete Cholesky-Conjugate Gradient method to solve the ground-water flow equation and the Line Successive Overrelaxation method to solve the solute-transport equation. A cylindrical coordinate finite-element grid was constructed to study the subsurface injection, storage, and recovery cycles in the Lower Floridan aquifer, and boundary and initial conditions were determined for the generalized model.

The calibration and testing of the model was performed by changing the model variables within realistic limits, until a satisfactory comparison between the observed and simulated solute breakthrough data was obtained. Satisfactory comparisons of simulated to observed dimensionless chloride concentrations for the deep monitor well were obtained when using the model during the injection and recovery phases of cycle 1, but not for the injection well during the recovery phase of cycle 1 even after several attempts. This precluded the determination of the recovery efficiency values by using the model. The cavernous or conduit nature of the Lower Floridan aquifer at the local scale permits very high velocities (relative to typical ground-water velocities) to develop near the injection well. Such velocities could explain the unsatisfactory comparisons of simulated to observed dimensionless chloride concentrations for the injection well and failure of the model to represent the field data at this well. To test this possibility, Reynolds numbers were estimated at varying distances from the injection well, taking into consideration two aquifer conceptual systems: porous media and cavernous.

For the porous media conceptual system, the square root of the permeability value was used as a characteristic length to estimate Reynolds numbers. The Reynolds numbers were greater than 10 at distances less than 1.42 m from the injection well. Thus, application of Darcy's law to ground-water flow might not be valid at this distance. At the deep monitor well located about 171 m from the injection well, the Reynolds number was about 0.08 which is representative of laminar porous media flow conditions.

For the cavernous conceptual system, the thickness (9 m) of high-permeability zone 1 was used as a characteristic length to estimate Reynolds numbers. The Reynolds numbers were greater than 2,000 at distances less than 1,000 m from the well. This number represents the upper limit of laminar flow, which is the fundamental assumption for the application of Darcy's law to free flow.

In conclusion, the simulation of recovery efficiency for the Lower Floridan aquifer at the Lake Okeechobee injection-well site might require the application of a free-flow type model (conduit flow or fracture flow model). This type of model may produce a more realistic representation of the actual fluid motion in the aquifer and will provide appropriate estimates of the recovery efficiency.

REFERENCES CITED

Bear, J., 1979, Hydraulics of groundwater: New York, McGraw-Hill, 569 p.

CH_2M Hill, 1989, Construction and testing of the aquifer storage recovery (A&R) demonstration project for Lake Okeechobee, Florida: Engineering Report, v. I.

Florida Department of Environmental Protection, 1993, Drinking water standards, monitoring and reporting: Chapter 17-550, Florida Administrative Code, 38 p.

Kipp, K.L., 1987, HST3D: A computer code for simulation of heat and solute transport in three-dimensional ground-water flow systems: U.S. Geological Survey Water-Resources Investigations Report 86-4095, 517 p.

Kuiper, L.K., 1987, Computer program for solving groundwater flow equations by the preconditioned conjugate gradient method: U.S. Geological Survey Water-Resources Investigations Report 87-4091, 34 p.

Lake Okeechobee Technical Advisory Committee, 1986, Final report: Tallahassee, Fla., Florida Department of Environmental Regulation.

Lukasiewicz, J., 1992, A three-dimensional finite difference ground water flow model of the Floridan aquifer system in Martin, St. Lucie, and eastern Okeechobee counties, Florida: South Florida Water Management District Technical Report 92-03, 292 p.

Merritt, M.L., 1985, Subsurface storage of freshwater in South Florida: A digital model analysis of recoverability: U.S. Geological Survey Water Supply Paper 2261, 44 p.

Merritt, M.L., Meyer, F.W., Sonntag, W.H., and Fitzpatrick, D.J., 1983, Subsurface storage of freshwater in south Florida: A prospectus: U.S. Geological Survey Water-Resources Investigations Report 83-4214, 69 p.

Meyer, F.W., 1989, Subsurface storage of liquids in the Floridan aquifer system in south Florida: U.S. Geological Survey Open-File Report 88-477, 25 p.

Miller, J.A., 1986, Hydrogeologic framework of the Floridan aquifer system in Florida and in parts of Georgia, Alabama, and South Carolina: U.S. Geological Survey Professional Paper 1403-B, 91 p.

Parker, G.G., Ferguson, G.E., Love, S.K., and others, 1955, Water resources of southeastern Florida, with special reference to the geology and ground water of the Miami area: U.S. Geological Survey Water-Supply Paper 1255, 965 p.

Puri, H.S., and Vernon, R.O., 1964, Summary of the geology of Florida and a guidebook to the classic exposures: Florida Geological Survey Special Publication 5, 312 p.

Quiñones-Aponte, Vicente, and Wexler, E.J., 1995, Preliminary digital simulation of injection, storage, and recovery of freshwater in the Lower Hawthorn aquifer, Cape Coral, Florida: U.S. Geological Survey Water-Resources Investigations Report 94-4121, 102 p.

Quiñones-Aponte, Vicente, Whiteside, D.V., and Zack, Allen, 1989, Single well injection and recovery of freshwater from an aquifer containing saline water in Arecibo, Puerto Rico: U.S. Geological Survey Water-Resources Investigations Report 88-4037, 19 p.

Quiñones-Aponte, Vicente, and Whitley, J.F., 1996 (in press), Testing phosphate removal by subsurface storage of canal water, mass balance: Ground Water.

Rouse, Hunter, 1956, Elementary mechanics of fluids: New York, John Wiley and Sons, 376 p.

Sellards, E.H., 1912, Soils and other surface residual material of Florida: Florida Geological Survey 4th Annual Report.

Tibbals, C.H., and Frazee, J.M., Jr., 1976, Ground-water hydrology of the Cocoa Well Field area, Orange County, Florida: U.S. Geological Survey Open-File Report 76-676.

Voss, C.I., 1984, A finite-element simulation model for saturated-unsaturated, fluid density-dependent groundwater flow with energy transport or chemically reactive single species solute transport: U.S. Geological Survey Water-Resources Investigations Report 84-4369, 409 p.

Young, D.M., 1954, Iterative method for solving partial differential equations of the elliptic type: Transactions American Mathematical Society, v. 76, p. 92-111.